A rapid and efficient screening system for neutralizing antibodies and its application for the discovery of potent neutralizing antibodies to SARS-CoV-2 S-RBD

Xiaojian Han[1,2,*], Yingming Wang[1,2,*], Shenglong Li[1,2,*], Chao Hu[1,2], Tingting Li[1,2], Chenjian Gu[3], Kai Wang [4], Meiying Shen[5], Jianwei Wang[1,2], Jie Hu[4], Ruixin Wu[1,2], Song Mu[1,2], Fang Gong[6], Qian Chen[1,2], Fengxia Gao[1,2], Jingjing Huang[1,2], Yingyi Long[1,2], Feiyang Luo[1,2], Shuyi Song[1,2], Shunhua Long[1,2], Yanan Hao[1,2], Luo Li[1,2], Yang Wu[3], Wei Xu[3], Xia Cai[3], Qingzhu Gao[4], Guiji Zhang[4], Changlong He[4], Kun Deng[7], Li Du[1,2], Yaru Nai[1,2], Wang Wang[1,2], Youhua Xie[3], Di Qu[3], Ailong Huang[4], Ni Tang[4#], Aishun Jin[1,2#]

[1]Department of Immunology, College of Basic Medicine, Chongqing Medical University, Chongqing, China

[2]Chongqing Key Laboratory of Basic and Translational Research of Tumor Immunology, Chongqing Medical University, Chongqing, China

[3]Key Laboratory of Medical Molecular Virology, Department of Medical Microbiology and Parasitology, School of Basic Medical Sciences, Shanghai Medical College, Fudan University

[4]Key Laboratory of Molecular Biology on Infectious Diseases, Ministry of Education, Chongqing Medical University, Chongqing, China

[5]Department of Breast Surgery, Harbin Medical University Cancer Hospital

[6]Yongchuan Hospital Affiliated to Chongqing Medical University

[7]The Third Affiliated Hospital of Chongqing Medical University, Chongqing, China

*These authors contributed equally to this work.

[#]Correspondence: aishunjin@cqmu.edu.cn (A.S.J) or nitang@cqmu.edu.cn (N.T.)

Abstract

Neutralizing antibodies (Abs) have been considered as promising therapeutics for the prevention and treatment of pathogens. After the outbreak of COVID-19, potent neutralizing Abs to SARS-CoV-2 were promptly developed, and a few of those neutralizing Abs are being tested in clinical studies. However, there were few methodologies detailly reported on how to rapidly and efficiently generate neutralizing Abs of interest. Here, we present a strategically optimized method for precisive screening of neutralizing monoclonal antibodies (mAbs), which enabled us to identify SARS-CoV-2 receptor-binding domain (RBD) specific Abs within 4 days, followed by another 2 days for neutralization activity evaluation. By applying the screening system, we obtained 198 Abs against the RBD of SARS-CoV-2. Excitingly, we found that approximately 50% (96/198) of them were candidate neutralizing Abs in a preliminary screening of SARS-CoV-2 pseudovirus and 20 of these 96 neutralizing Abs were confirmed with high potency. Furthermore, 2 mAbs with the highest neutralizing potency were identified to block authentic SARS-CoV-2 with the half-maximal inhibitory concentration (IC_{50}) at concentrations of 9.88 ng/ml and 11.13 ng/ml. In this report, we demonstrated that the optimized neutralizing Abs screening system is useful for the rapid and efficient discovery of potent neutralizing Abs against SARS-CoV-2. Our study provides a methodology for the generation of preventive and therapeutic antibody drugs for emerging infectious diseases.

Introduction

Pandemic outbreaks of infectious diseases, such as three novel pathogenic human coronaviruses in the past two decades: severe acute respiratory syndrome coronavirus 2 (SARS-CoV-2), middle eastern respiratory syndrome coronavirus (MERS-CoV) and SARS-CoV, have caused high mortality and unprecedented social and economic consequences[1-4]. While vaccines are effective in blocking infectious diseases, antibody therapy is an alternative treatment strategy for preventing newly emerging viruses. During the outbreaks of SARS-CoV, MERS-CoV and SARS-CoV-2, convalescent plasma from these patients containing neutralizing mAbs was a safe and effective treatment option to reduce mortality in severe cases[5,6]. However, convalescent plasma are limited and polyclonal non-neutralizing Abs in the plasma may cause undesired side effects[7]. The neutralizing mAbs therapeutics are effective replacements of convalescent plasma therapy. A rapid and efficient neutralizing Abs screening method against infectious diseases is in great needs.

The outbreak of COVID-19 was caused by SARS-CoV-2. Its viral spike(S) containing the receptor-binding domain (RBD) is responsible for binding to the receptor angiotensin-converting enzyme-2(ACE2) receptor on the host cells[8,9]. To date, several teams have promptly developed some potent neutralizing mAbs to SARS-CoV-2[10-22]. In these studies, different methodologies were employed for screening of neutralizing Abs. Some studies utilized SARS-CoV-2 S - or RBD- labeled memory B cells from convalescent patients with SASR-CoV-2 infection and directly amplified Ab genes by RT-PCR and nested PCR at a single-cell level[10,18]. In other studies, plasma cells were activated and expanded with stimulators and cytokines in vitro for selecting neutralizing Abs[14,19]. Humanized mice were also used to generate full human monoclonal antibodies against S protein[11,22]. Furthermore, using single-cell sequencing technology in combination with the enrichment of antigen-specific B, some researchers quickly detected thousands of antigen specific mAbs sequences[17,21]. Although these studies showed that neutralizing antibodies against SASR-CoV-2 could be obtained from convalescence patients, few methodologies were reported in detail about how to generate neutralizing Abs of interest rapidly and efficiently.

Here, we describe a strategically optimized system for fast screening of neutralizing mAbs to achieve efficient and reliable yield of desired neutralizing Abs in as short as 6 days. A total of 198 Abs against RBD of SARS-CoV-2 were obtained with this method, and 50% of them were potential candidate neutralizing Abs in a preliminary screening of pseudovirus system. Furthermore, 20 of these neutralizing

mAbs are confirmed with high potency, and 2 mAbs reached IC_{50} in nanogram range. Therefore, the screening system can generate a large number of neutralizing mAbs for the discovery of potent antibody drugs, providing vital information to understand the characteristics of new viruses, and, collectively, to develop preventative and therapeutic strategies for newly emerging infectious diseases in the future.

Results

Establishment of a rapid and efficient neutralizing Abs screening system. Previously we had obtained specific mAbs from PBMC of vaccinated volunteers via microwell array chips within only one week [23]. Here, we established the optimized screening system based on the memory B cells from the PBMC to obtain neutralizing mAbs rapidly and efficiently (Figure 1). At first, we collected the blood samples and isolated the PBMC from a panel of Chinese convalescent patients infected with SARS-CoV-2 in February. RBD specific memory B cells (mB cells) in a pooled PBMC from 5-7 blood samples were detected by labeling with RBD. RBD-specific mB cells were sorted into 96-well PCR plates in a single-cell manner. Each single-cell Ab cDNA was amplified, and the immunoglobulin heavy (IGH) and light chains (IGK and IGL) of the variable region were obtained by RT-PCR and nested PCR with the optimized primers at Day 1 (Table S4. Primers List of BCR PT-PCR). Recombinant sites were introduced by the nested primers during the 2nd PCR. Next, linear antibody gene expression cassettes were assembled by overlapping PCR, which contained the essential elements for Ab gene transcription, including the CMV promoter, the antibody variable region, the constant region and the poly(A) tail. Then HEK293T cells were transiently transfected with these linear antibody gene expression cassettes, for the expression of recombinant antibodies at Day 2. Culture supernatants of the transfected cells were evaluated for the S and RBD specific binding activity by enzyme-linked immunosorbent assays (ELISA) at Day 4, and their pseudovirus neutralizing capacity was tested in HEK293T/hACE2 cells at Day 6. The screening system allowed us to harvest a large number of potential neutralizing Abs against SARS-CoV-2 within only 6 days. Furthermore, recombinant antibody proteins of interest were expressed and purified for subsequent functional analysis, including antibody specific binding ability, viral neutralization and antigen-binding affinity, all of which were completed with an additional 9 days.

Compared with conventional methods for screening neutralizing Abs[10,13,14,17,21], a few strategically optimized details of our screening system were described as following (Figure S1. The optimization of the screening platform). First, we collected the blood samples from convalescent patients with COVID-

19. These patients were the earliest confirmed cases of SARS-CoV-2 infection in Chongqing City, over half of the patients who had a history of close contact with the earliest infectors. Antigen specific B cells from memory B cells experienced affinity maturation and somatic hypermutation[24,25]. Thus, RBD specific memory B cells in these patients were potentially useful candidates to screen out the potent neutralizing Abs. Second, we sorted the $CD19^{+}IgD^{-}IgG^{+}$ memory B cells in the pooled PBMC samples from multi-patients to achieve a higher probability in antibody diversity. We then utilized RBD of SARS-CoV-2 as the bait to label the specific memory B cells. Removing dead cells was essential for sorting of the relatively rare RBD specific mB cells, which only occupied less than 1% of $CD19^{+}IgD^{-}$ IgG^{+} memory B cells (Figure S2. The influence of dead cells on the sorting of RBD-specific memory B cells). Additional improvements were applied to the single-B cell receptor (BCR) cloning[26,27] and expression (Figure S3. Schematic diagram of BCR RT-PCR and linear expression cassettes construction). We chose the initial 20 nucleotides located at 5' end of the signal peptide in Ab genes as the forward primers in the 1^{st} PCR step, and the adaptor primer in the 2^{nd} PCR step. This was beneficial for reducing potential loss of BCR clones caused by SNP at the primer binding sites. Besides, the 2^{nd} PCR products containing the adaptor primer could be used for the simultaneous construction of linear gene expression cassettes and plasmids without the extra-modification. with Ab J-region primers in the 2^{nd} PCR, we are able to improve the recombination efficiency of linear cassettes approaching 100%. Our strategy of linear gene cassettes skipped the process of plasmid construction, which could reduce time-consuming procedures and labor, and be more suitable for a large scale of antibody screening[28] (Table S6. The annotation of linear antibody expression cassettes). Taken together, we optimized a methodology for the rapid and efficient identification of neutralizing Ab candidates (Figure S3A, Table S3-S6).

Detection and isolation of RBD specific memory B cells. To apply our established screening system of neutralizing Abs, we collected the plasma and PBMC from 39 convalescent patients with COVID-19 admitted to Chongqing Medical University affiliated Yongchuan Hospital (Table S1. Patient Information). These convalescent plasma had been preliminarily screened for positive virus-specific binding and neutralization capacity, using a magnetic chemiluminescence enzyme immunoassay (MCLIA) and a pseudovirus-based assay[29]. Using ELISA assay, we confirmed that those Abs targeting Spike or recombinant RBD of SARS-CoV-2, SARS-CoV, and MERS-CoV in the plasma with 10-fold dilution. Among these convalescent patient samples, 36 plasma showed high reactivity to SARS-CoV-2 S or RBD proteins, while the other three patients had weak reactivity to these antigens (Figure 2A). Almost all

samples had cross-reactivity to the S1 protein of SARS-CoV and MERS-CoV with 10- or 100-fold dilution, while the healthy donor's plasma react to none of these three coronaviruses (Figure 2A). With these findings, we felt confident that all samples could be used for the specific mAb isolation.

Since RBD is the key domain for the SARS-CoV-2 S protein to interact with human cell surface ACE2 receptor, the recombinant RBD was employed to detect the specific memory B cells via flow cytometry. We analyzed RBD-specific memory B cells by a gating strategy of Dead_Dye-$CD19^{+}IgG^{+}IgD^{-}$ RBD^{+}cells (Figure 2B), the proportion of which was less than 1% in $IgD^{-}IgG^{+}$ memory B cells (ranging from 0.1% to 0.33%, Figure 2C). These RBD-specific mB cells were then sorted into 96-well plate one cell per well for Ab gene isolation. Immunoglobulin heavy and light chains were amplified by nested PCR from the sorted single mB cells (Figure S3B). The amplified products were cloned into linear expression cassettes to produce full-length IgG1 antibodies (Figure S3B). After three rounds of screening, a total of 497 paired heavy chains and light chains of Ab genes were obtained from the sorted RBD-specific memory B cells (Table S2. Three batches of S-RBD specific B memory cell sorting).

Specificity and neutralization of Abs expressed by linear expression cassettes. The amplified products with heavy chains and light chains of Ab genes were separately cloned into linear expression cassettes. We then transfected HEK293T cells with these linear expression cassettes to identify the specificity of these Abs. Antibodies within the supernatant of transfected HEK293T cells were screened by ELISA for their binding capability to the recombinant S1 and RBD protein of SARS-CoV-2. In total, we identified 198 RBD specific antibody genes from the 497 pair Ab genes (Figure 3A). To assess the neutralization ability of these specific antibodies, we used pseudovirus bearing SARS-CoV-2 S protein to infect 293T/hACE2 cells. Interestingly, 96 out of 198 antibodies (48.5%) showed the potential ability to block pseudovirus with an inhibitory rate of over 75% (Figure 3A), suggesting that RBD region was an ideal candidate to screen neutralizing Abs for blocking SARS-CoV-2. These results demonstrated that our screening system can rapidly and efficiently screen neutralizing Abs using patients' specific memory B cells.

Sequence analysis for the diversity of RBD-specific Abs. We then successfully sequenced 169 RBD-specific Abs. Among them, 158 (93.5%) Abs had unique patterns of distribution with various gene clusters (Figure S4. Usage and pairing of heavy and light chain for all specific antibodies). We also analyzed the distribution of heavy chain and light chain gene clusters according to neutralizing capability of mAbs tested by pseudovirus assays, as shown in Figure 3B and Figure S4A. Abs with neutralizing

rate over 75% to block pseudovirus were termed as potential neutralizing Abs (pote-nAbs). The almost sequenced Abs were transcribed from the IGHV1-IGHV5 for the heavy chain and IGKV1-IGKV3 and IGLV1-IGLV3 for light chain (Figure S5). We found that close to 50% of the pote-nAbs were specifically transcribed from IGHV3 for the heavy chain, and from IGKV1 for the light chain (Figure S5. Phylogenetic analysis of VH (up) and VL (down) genes for RBD-binding antibodies). Interestingly, we found that all mAbs encoded by IGHV3-66 were pote-nAbs (Figure 3B), and the IGHV3-66 family paired with IGKV1-33, IGKV1-9 and IGLV1-40 (Figure S4C). Additionally, a large number of mAbs encoded by IGKV1-39 were pote-nAbs (Figure S4A). Of note, we found that IGKV1-39 gene cluster also paired with a bundle of heavy chains to express RBD specific mAbs (Figure S4C), which was consistent with previous reports [11,19].

The heavy chain complementarity determining region 3 (CDRH3) is the most variable region of an antibody in amino acid compositions and lengths. The average length of CDRH3 in the naive human repertoire is round 15 amino acids with a normal distribution[30]. We observed that the CDRH3 lengths of the specific mAbs were mainly distributed between 11-19 amino acids, while the overall CDRH3 lengths matched the skew distribution (Figure 3C). Most of the potent-Abs contained 11-16 amino acids (Figure 3C). The mean CDRH3 length of isolated SARS-CoV-2 S-RBD-specific mB cells differs substantially from that of other viral infections, such as HIV and influenza virus[31,32]. In terms of the CDR3 light chain (CDRL3) lengths, a range of 6 to 13 amino acids were observed, with similar skew distribution (Figure S4B).

Potent neutralizing ability and antigen affinity of mAbs. The variable regions of potential neutralizing Abs were cloned into antibody expression vectors to construct Ab plasmids. We successfully harvested 73 purified mAbs, from a total of 96 potential neutralizing mAbs that were produced by transfecting Expi293F cells. When we tested the specificity of purified mAbs by ELISA, we found 65 Abs that formed tight interaction with SARS-CoV-2 S1 and SARS-CoV-2 RBD (Figure 4A). Next, these mAbs were assessed with RBD-ACE2 interaction blocking assay to confirm their neutralizing ability *in vitro*. We found that 71% of them could block the interaction between ACE2 and RBD (Figure 4B).

Forty-eight purified mAbs were evaluated for their neutralizing potency using the authentic SARS-CoV-2 cytopathic effect (CPE) inhibition assay, and the results were listed according to the order of inhibitory potency (Figure 5A). We successfully obtained a total of 20 antibodies that were able to completely block the authentic SARS-CoV-2 infection with the concentrations of 1 μg/ml. The top level 2 mAbs on the

list were termed as the most potent neutralizers (completely inhibition < 0.14 μg/ml), and another 18 mAbs as the moderate neutralizers (0.29-1.17 μg/ml). The IC_{50} of the most potent neutralizers (58G6, 510A5) were determined by RT-qPCR method using authentic SARS-CoV-2 virus infection. We found that the IC50 values of 58G6 and 510A5 were 9.98 ng/ml and 11.13 ng/ml, respectively (Figure 5B). Therefore, we tested the binding affinity of 58G6 and 510A5 to SARS-CoV-2 S-RBD via the surface plasmon resonance (SPR) assay. The measured equilibrium constant (Kd) of 58G6 with SARS-CoV-2 S-RBD was 0.385 nM and that of 510A5 was 7.8 nM, respectively (Figure 5C). In our study, 58G6 and 510A5 are the best mAsb with potent neutralization and high affinity against SARS-CoV-2.

Discussion

Neutralizing antibodies were considered as an ideal medicine for prophylaxis and treatment of infectious diseases[33]. At present, several potent neutralizing Abs to SARS-CoV-2 have been promptly developed and being tested in clinical trials (clinicaltrials.gov NCT04497987, NCT04426695 and NCT04425629) for treating COVID-19 patients [12-15,17,19-21,34,35]. These reports showed that even though neutralizing antibodies against SASR-CoV-2 could be obtained from convalescent patients, the success rate to discover potent neutralizing antibodies with therapeutic value remains unideal. In this study, we described a strategically optimized screening method to discover potent mAbs from a large number of potential neutralizing Abs.

In general, here is how researchers obtain neutralizing antibodies. Blood samples were collected from convalescent patients with SASR-CoV-2 infection, and PBMC were separated in order to isolate SASR-CoV-2 specific B cells. Then the paired heavy and light chain sequences of Ab genes were obtained either in a single-cell PCR manner[10,12,15,18], or directly by high-throughput single-cell sequencing[17,21]. In our study, we obtained the paired Ab genes at the single-cell level, and optimized steps of a screening workflow for neutralizing Abs, we were able to obtain the most potent neutralizing Abs with high speed and efficiency.

Firstly, we optimized the specificity of antibody isolation to increase target neutralizing Abs probability. Because the key sites of RBD have been clearly demonstrated to be essential for ACE2 binding during SARS-CoV-2 entry[8,36], we chose to sort RBD-specific memory B cells for the isolation of heavy and light chains. It has been evidenced that RBD-specific neutralizing Abs can inhibit SARS-CoV-2 entry to host cells[10], we have observed similar findings with psudovirus infection (Figure 3). Recent reports have

219 demonstrated that when SARS-CoV-2 S was used as bait to label antigen-specific mB cells, it could
220 result in a large of undesired antibodies against over-broad antigenic sites belonging to non-RBD
221 regions[12,17]. When we used RBD as bait to isolate antibodies from mB cells, we found the obtained mAbs
222 were more effective in blocking authentic viruses (Figure 5), which might largely due to the fact that
223 RBD was enriched with the ACE2 binding epitopes.
224 Secondly, we optimized multiple steps to improve the efficiency of nAb screening. This has been
225 achieved by smarter primer design, application of linear expression cassettes and preliminary
226 neutralization assay to exclude non-neutralizing Abs, and these will be discussed in detail. Initially, we
227 designed primers targeting the initial 20 nucleotides at the 5' end of the signal peptide of Ab genes as the
228 forward primers in the 1st PCR step. This can reduce the loss of BCR clones caused by SNP at the primer
229 binding sites. Also, we added an adaptor primer in the 2nd PCR step. Such adaptor with the same
230 sequences as downstream recombination sites was convenient for the next PCR and recombinant
231 plasmids construction, which could be suitable for high-throughput screening of specific Abs. Next, we
232 successfully constructed linear expression cassettes with heavy chains or light chains, to rapidly identify
233 the specificity of Abs. Construction of the linear expression cassettes was much easier than plasmids,
234 which could drastically reduce the workload and time. Moreover, the linear Ab gene expression cassettes
235 expressed in the cell supernatants of HEK293T cells were evaluated for neutralization activity on the
236 sixth day. Neutralizing Abs account for approximately 50% of RBD-specific Abs, as shown in Figure
237 3A. By detecting the ability of purified mAbs to block the interaction of RBD with ACE2, we could filter
238 out only those Abs with neutralizing activities, to be applied in the subsequent steps. Together, these
239 optimizations allowed us to finish one round of the screening for neutralizing Abs in, as short as, 15 days.
240 The details of this optimized steps of our established methodology are shown (Figure S3, Table S03~S05).
241 Thirdly, we used both authentic SARS-CoV-2 cytopathic effect (CPE) inhibition assay and quantitative
242 analysis by RT-qPCR to ensure the accuracy of our findings, which lead to the successful identification
243 of 20 potent neutralizing antibodies that can completely block authentic virus infection, at concentrations
244 1.17 μg/ml. And the top two antibodies (58G6 and 510A5) generated IC_{50} values at around 10 ng/ml,
245 which were, as far as we know, two of the most potent neutralizing mAbs discovered to date.
246 Last but not least, we reduced duplicating clones by sample selection and increased the efficiency of
247 BCR cloning by adjusting gating strategy. It has been reported that substantial mAbs clones to SARS-
248 CoV-2 expanding in the individual patient sample is relatively common[13,18]. In our study, almost all RBD-

specific mAb clones were different from one another, while the proportion of clonal expansion was only 6.5% in all sequences, as compared to approximately 20%[13,18]. It could result from our pooled PBMC for sorting RBD-specific memory B from 5-7 convalescent COVID-19 patients. Therefore, it is beneficial to improve sample selection by methods that can best yield diverse mAbs of interest. Furthermore, RBD-specific memory B cells were mainly sorted after removing dead cells, this process increased the efficiency of BCR cloning.

Such optimized screening system allowed us to efficiently generate a panel of neutralizing Abs with relatively great potency. When we analyzed the distribution of gene clusters of B cell receptor (BCR) repertoire of abundant potential neutralizing and non-neutralizing antibody sequences, a few interesting observations were found. Our results revealed that potential neutralizing Abs tended to be distributed in several gene clusters, such as VH3-66 and VH3-53 allele, etc., among which, the VH3-66 has exclusively produced neutralizing Abs. This result may be helpful in analyzing the preference distribution of neutralizing Abs in the future. Meanwhile, CDRH3 length is reported as a key factor to value the diversity of RBD specific Abs, due to the changeable amino acid composition. We found that the CDRH3 length of potential neutralizing Abs showed a skewed distribution, with an inclined length of 11-16 amino acids. It suggested that the SARS-CoV-2 antibodies were likely derived from memory B cells during the primary response to SARS-CoV-2 infection but not a recall response to SARS-CoV or MERS, even though our collected blood specimens were cross-reactive with both SARS-CoV and MERS S protein[32]. One additional improvement that can be integrated into our screening system is single-cell sequencing. The development of proper algorithms for neutralization evaluation with incorporation of heavy chain variable region preferences, for example, IGHV3-66, could help to precisely predict neutralizing antibody from thousands of antigen specific mAbs repertoire[17,21]. This might further provide desired candidates of neutralizing Abs with potential therapeutic value, with better time-efficiency and economical preferences.

In conclusion, we have successfully established a strategically optimized screening system of neutralizing antibodies that can generate ideal numbers of neutralizing Abs in a total period of 15 days. This methodology can open the way for the potential on-time therapeutic applications towards various emerging pathogens in the future.

Materials and Methods

Isolation of single RBD-specific memory B cells by FACS. PBMCs from the convalescent patients were thawed and rested overnight. The mixed samples staining as following. 2 μg/ml RBD-his in 200 μl PBS (added with 2% FBS) was mixed with the specific antibody cocktail required for staining B cell. Then these PBMCs was incubated with mixed antibodies cocktail at 4 °C for 30 min (the antibodies cocktail including FITC-anti-human CD19 antibody (Biolegend, clone: SJ25C1), BV421-anti-human IgD antibody (Biolegend, clone: IA6-2), PerCP-Cy5.5-anti-human IgG antibody (Biolegend, clone: M1310G05), APC-anti-his tag antibody (Biolegend, clone: J095G46)). Dead dye (LIVE/DEAD™ Fixable Near-IR Dead Cell Stain Kit, Thermo Fisher) was added at 4 °C for 20 min. After washing the cells, the FACS analysis were performed by BD FACSAriaIII (BD Biosciences) with FSC-A versus SSC-A identifying cell population, FSC-A versus FSC-H excluding doublets. Then FSC-H versus Dead Dye was gated to remove dead cells. RBD-specific single memory B cells were gated by $CD19^{+}IgD^{-}IgG^{+}His^{+}$, and single-cell sorted into 96-well PCR plates (free of DNase and RNase, Bio-Rad). The Plates were stored at -80 °C until BCR Cloning. Data analysis was performed utilizing the FlowJo software (FlowJo, LLC).

Amplification of single-cell BCR variable region. Our primers for PCR were designed from leader sequences and J region sequence of immunoglobulin (Ig) annotated by the IMGT reference directory (http://www.imgt.org/vquest/refseqh.html). An adaptor sequence was added to the 5′ end of the leader primers for the 2nd PCR. 31 leader primers (AP_G_leader Mix) was designed for the heavy chain of Ig, and 19 leader primers (AP_K_leader Mix) was used in the amplification of the kappa chain of Ig, and 21 leader primers (AP_L_leader Mix) for the lambda chain of Ig were designed. For the initial step of RT-PCR, 5 μl of the RT_Mix_A was added into each well of 96 well plate containing a single B cell. Then the mixture was incubated at 65℃ for 5 min and put on ice immediately for 3 min. 5 μl RT_Mix_B was added into each well of the plate with reaction program: 45 ℃ for 45 min, 70 ℃ for 15 min. 1 μl of RT product was moved to the well of a new 96 well plate containing 9 μl 1st_PCR_Mix_Gamma /Kappa/Lamda, respectively. The PCR program for 1st PCR: 95℃ for 3 min, 30 cycles of 95℃ for 10 sec, 55℃ for 5 sec and 72℃ for 1 min. 1 μl of the tenfold-diluted 1st PCR product was then added into each well of a new 96 well plate holding 9 μl 2nd PCR_Mix_Gamma/Kappa/Lamda, respectively. The PCR program for 2nd PCR: 95℃ for 3 min, 35 cycles of 95℃ for 10 sec, 55℃ for 5 sec, and 72℃ for 45 sec. The second PCR products were further cloned into the antibody linear expression cassettes or expression vectors to express full IgG1 antibodies. PCR reaction Mix are prepared as described in Table

S3. All of the PCR primers are listed in Table S4 and prepared in Table S5.

Generation of linear antibody expression cassettes and expression of Abs. 2nd PCR products were used to ligate with the expression cassettes directly by overlapping PCR. The products were purified with ethanol precipitation method. Briefly, 120 µl of absolute ethanol and 6 µl of 3 M sodium acetate were mixed with 60 µl of the Overlap PCR product. Then the reagents were incubated at -80 °C for 30 minutes. After centrifuging at 10,000 rpm for 20 minutes, the supernatant was discarded the and the pellet adhered on the tube were rinsed with 200 µl 70% ethanol and absolute ethanol and evaporated the ethanol at 56°C for 10 min. 40 µl sterile water was added to dissolve the DNA pellet. After measuring the nucleic acid concentration, purified overlapping PCR products of paired heavy and light chain expression cassettes were co-transfected in HEK293T cells. The binding ability of transfected culture supernatants to SARS-CoV-2 S-RBD was tested by ELISA after 48 hours.

Recombinant antibody production and purification. For the construction of antibody expression Vectors, VH and VL 2nd PCR products were inserted separately into the linearized plasmids (pcDNA3.4) that encode constant regions of the heavy chains and light chains via a homologous recombination kit (Catalog No. C112, Vazyme). A pair of plasmids separately expressing heavy and light chain of antibodies were transiently co-transfected into Expi293™ cells (Catalog No. A14528, ThermoFisher) with ExpiFectamine™ 293 Reagent. Then the cells were cultured in shaker incubator at 120 rpm and 8% CO_2 at 37 °C. After 7 days, the supernatants with the secretion of antibodies were collected and captured by protein G Sepharose (GE Healthcare). The bound antibodies on the Sepharose were eluted and dialyzed into phosphate-buffered saline (PBS). The purified antibodies were used in following binding and neutralization analyses.

ELISA binding assay and competitive ELISA. 2 µg/ml the recombinant S or RBD proteins derived from SARS-CoV-2, SARS-CoV, or MERS-CoV (Sino Biological, Beijing) were coated on 384-well plates (Corning) at 4°C overnight. Plates were blocked with blocking buffer (PBS containing 5% FBS and 2% BSA) at 37°C for 1 hour. Serially diluted convalescents' plasma or mAbs were added into the plates and incubated at 37°C for 30 min. Plates were washed with phosphate-buffered saline, 0.05% Tween-20 (PBST) and ALP-conjugated goat anti-human IgG (H+L) antibody (Thermo Fisher) was added into each well and incubated at 37°C for 1 hour. Lastly, the PNPP substrate was added, and absorbance was measured at 405 nm by a microplate reader (Thermo Fisher). For a competitive ELISA to test the effect of mAbs on blocking ACE2 binding RBD, 2 µg/ml the recombinant ACE2 (Sino Biological,

Beijing) was added in 384-well plates and overnight at 4°C, followed by blocking with the blocking buffer and washing. 500 ng/ml RBD-mouse-Ig-Fc was pre-incubated with test specimen at 37°C for 1 hour, followed by adding into the wells coated with ACE2 and incubated at 37°C for 1 hour. Unbound antigen were removed with washes. Then ALP-conjugated anti-mouse-Ig-Fc antibody was added into the wells and incubated at 37°C for 30 min. PNPP was added and measured as above.

Pseudovirus neutralization assay. Pseudovirus was generated as previously described[37,38]. HEK293T cells were transfected with psPAX2, pWPXL Luciferase, and pMD2.G plasmid encoding either SARS-CoV-2 S. The supernatants were harvested 48 hours later, filtered by 0.45 μm filter and centrifugated at 300 g for 10 min to collect the supernatant and then aliquoted and storied at -80°C. The purified antibodies with serial dilution were incubated with pseudovirus at 37°C for 1 hour. The mixture of viruses and specimens was then added in a hACE2 expressing cell line (hACE2-293T cell). After 48 hours culture, the luciferase activity of infected hACE2/293T cells was measured by the Bright-Luciferase Reporter Assay System (Promega). Relative luminescence units (RLU) of Luc activity was detected using ThermoFisher LUX reader. All experiments were performed at least three times and expressed as means ± standard deviations (SDs). Half-maximal inhibitory concentrations (IC_{50}) were calculated using the four-parameter logistic regression in GraphPad Prism 8.0.

Authentic SARS-CoV-2 virus neutralization assays. An authentic SARS-CoV-2 neutralization assay was performed in a biosafety level 3 laboratory of Fudan University. Serially diluted mAbs were incubated with authentic SARS-CoV-2 (nCoV-SH01, GenBank: MT121215.1, 100 TCID50) at 37°C for 1 hour. After incubation, the mixtures were then transferred into 96-well plates, which were seeded with Vero E6 cells. After incubation at 37°C for 48 hours, each well was examined for CPE and supernatant viral RNA by RT-qPCR. For RT-qPCR, the viral RNA was extracted from the collected supernatant using Trizol LS (Invitrogen) and used as templates for RT-qPCR analysis by Verso 1-step RT-qPCR Kit (Thermo Scientific) following the manufacturer's instructions. PCR primers targeting SARS-CoV-2 N gene (nt608-706) were as followed (forward/reverse):5′-GGGGAACTTCTCCTGCTAGAAT-3′/5′-CAGACATTTTGCTCTCAAGCTG-3′. qRT-PCR was performed using the LightCycler 480 II PCR System (Roche) with program as followed: 50°C 15 min; 95°C 15 min; 40 cycles of 95°C 15 sec, 50°C 30 sec, 72°C 30 sec.

Antibody binding affinity measurement by SPR. The affinity of antibody binding SARS-Cov-2-S-RBD was measured via the Biacore X100 platform. The CM5 chip (GE Healthcare) was coupled with

an anti-human IgG-Fc antibody to capture 9000 response units antibodies. Gradient concentrations of SARS-Cov-2-S-RBD (Sino Biological Inc.) were diluted (2-fold dilution, from 50 nM to 0.78 nM) with HBS-EP^{+} Buffer (0.01 M HEPES, 0.15 M NaCl, 0.003 M EDTA and 0.05% (v/v) Surfactant P20, pH 7.4), then injected into the human IgG capturing chip. The sensor surface was regenerated with 3 M magnesium chloride at the end of each cycle. The affinity was calculated using a 1:1 binding fit model in Biacore X100 Evaluation software (Version:2.0.2).

Sequence analysis of antigen-specific mAb sequences. IMGT/V-QUEST (http://www.imgt.org/IMGT_vquest /vquest) and IgBLAST (https://www.ncbi.nlm.nih.gov/igblast/), MIXCR (https://mixcr.readthedocs.io/en/master/) and VDJtools (https://vdjtools-doc.readthedocs.io/en/master/overlap.html) tools were used to do the VDJ analysis and annotation, germline divergence for each antibody clone. The Phylogeny tree analysis of IgG heavy and light chain variable genes was performed with MegaX (Molecular Evolutionary Genetics Analysis across computing platforms) by the Maximum Likelihood method. Abs DNA sequences were compared with each other by ClustalW (pairwise alignments) to analyze sequence similarity, and EvolView (https://www.evolgenius.info/evolview/) was used for the decoration of Phylogeny tree. R packages (ggplot2, pheatmap) were used for the bar chart, heatmap and Cicos plot.

Ethics Statement. The project “The application of antibody tests patients infected with SARS-CoV-2” was approved by the ethics committee of ChongQing Medical University. Informed consents were obtained from all participants.

Acknowledgments: We acknowledge the work and contribution of blood sample providers from Chongqing Medical University affiliated Yongchuan Hospital and the third affiliated Hospital of Chongqing Medical University. We also thank health donors from Chongqing Medical University. This study was supported by Chongqing Medical University fund (X4457) with the donation from Mr Yuling Feng.

Author contributions

AJ, AH conceived and designed the study, KD, CH, LD, YN offered help on collection of convalescent patient blood samples. Most of the experiments were completed by XH,TL, CH, YW, JW, RW, FG, JH, SM, YL, FL, SS, YH, QC, LL with the assistance from TN, YX, CG, HJ, YW, WX, XC, QG, GZ, CH, WK. SL, MS, YW, XH, AJ played an import role in data analysis of neutralizing Abs sequences. SL,

MS, YW, JW performed to generated figures and tables and take responsibility for the integrity and accuracy of data presention. AJ, XH wrote the manuscript and SL, TL, JW and YW helped to revise it.

Data availability statements All information presented in this study will be upload soon.

Conflict of interests: We declare no competing financial interest.

403 **Figure legends**

404 **Figure 1. Schematic model depicting a rapid and efficient screening system of neutralizing Abs.**
405 Rapid neutralizing antibody screening workflows and timelines are shown, representing the multiple
406 workflows conducted in parallel. PBMC were isolated from collected convalescent patients' blood, and
407 the RBD-specific memory B cells in the PBMCs were sorted as single-cell via flow-cytometric sorter
408 (day 1). Then, the IgG heavy and light chains of monoclonal antibody genes were amplified by RT-PCR
409 on the same day. 2nd PCR products were cloned into linear expression cassettes on the second day.
410 Antibodies were expressed by transient transfection with equal amounts of paired heavy and light chain
411 linear expression cassettes in HEK293T cells and culture for two days. The cell supernatants in
412 HEK293T cells were detected for the specificity of antibodies by ELISA in 384-well plates on the fourth
413 day. The neutralizing activity of antibodies was detected with pseudovirus bearing SARS-CoV-2 S in
414 96-well plates on the sixth day. The potential neutralization antibody expression plasmids were
415 transfected into Exi293F cells for large-scale production of Ab proteins. The cell supernatants in Exi293F
416 cells were collected, and antibody proteins were purified by protein G. They were further measured for
417 the binding ability and neutralizing activity via ELISA and competitive ELISA *in vitro*. Additionally,
418 virus neutralization assay was performed. Created with Biorender.com.

419

420 **Figure 2. Isolation of RBD-specific memory B cells using flow cytometry. A.** The heatmap depicts
421 the specificity of convalescent patients' plasma against S1 and RBD from SARS-CoV-2, SARS-CoV
422 and MERS-CoV, measured by ELISA. Serial dilutions of plasma samples were performed to test the
423 reactivity of antibodies in plasma. The plasma of healthy donors was used as the control. Data were
424 shown with the mean of representative experiments. **B.** Gating strategy for SARS-CoV-2 RBD-specific
425 IgG^+ B cells in PBMCs of the convalescent patients. Living $CD19^+$ IgD^-IgG^+ cells were gated, and cells
426 with positive SARS-CoV-2 RBD staining were selected for single-cell sorting. **C.** FACS analysis of
427 RBD-specific memory B cells in $CD19^+IgD^-IgG^+$ memory B cells from PBMCs of three batch
428 convalescent patients. Plots show $CD19^+IgD^-IgG^+RBD^+$ populations using gating strategy described in
429 **B.**

430

431 **Figure 3. Identification of RBD specific monoclonal antibodies from convalescent COVID-19**
432 **patients. A.** Screening of specific Abs against SARS-CoV-2 S1 and RBD. The heatmap reveals that the

binding ability of 198 Ab supernatants produced by HEK239T cells transfected with linear Ab gene expression cassette. The mAbs rank as the screening sequence, and binding activity of mAbs against SARS-CoV-2 S1 and RBD were tested by ELISA. The brightness of blue represents the binding strength, which reflected the $OD_{405\ nm}$ value tested by ELISA. The neutralizing activity of mAbs was discriminated according to the neutralizing value. Antibody-mediated blocking of luciferase-encoding SARS-CoV-2 typed pseudovirus transfected into hACE2/ HEK293T cells were measured by values of relative light units（RUL）. The Green columns indicate potential neutralization (neutralizing activity >75%), while white indicate partial or not neutralization (neutralizing activity <75%). **B.** Frequencies of variable region of heavy chain (VH) gene clusters for potential neutralizing and non-neutralizing antibodies. Clonal sequences groups were collapsed and treated as one sample for calculation of the frequencies. **C.** Frequency of various the heavy chain complementarity determining region 3 (CDRH3) length of in potential neutralizing and non-neutralizing antibodies.

Figure 4. The binding activity and inhibition of ACE2-RBD interaction of mAbs tested by ELISA and competitive ELISA. A. The $OD_{405\ nm}$ value refects a binding strength of purified mAbs to 1 μg/ml SARS-CoV-2 S1 or RBD. Plates were coated with recombinant S1 or RBD protein of SARS-CoV-2, then incubated with purified mAbs. A SARS specific mAb (CR3022) was set as the positive control. The blue dashed lines indicated the OD_{405nm} value of a negative sample. **B.** The inhibitory effect of purified mAbs against the interaction between SARS-CoV-2 RBD and hACE2 was tested via competitive ELISA analysis. Blocking efficacy was determined by comparing response units with and without prior antibody incubation. The green dashed lines indicated 50% inhibition on blocking the interaction ACE2 and RBD interaction.

Figure 5. Functional characteristics of neutralizing Abs against SARS-CoV-2. A. Neutralization activity of mAbs against authentic SARS-CoV-2 virus (nCoV-SH01) were analyzed by Cytopathic effects (CPE) test. Serial dilutions of mAbs were tested in parallel against authentic SARS-CoV-2, ranging from 18.76 μg/ml to 0.14 μg/ml. CPE results was summarized in (A) where "++++" indicates 100% cytopathy, "+++" indicates 50-75%, "++" indicates 25-50%, "+" indicates <25% and "-" indicates no cytopathy. 13G9 was marked "*", which was obtained by the method previously described[23]. **B.** The neutralization activity of 58G6 and 510A5 against the authentic SARS-CoV-2 virus was determined in

Vero-E6 cells by RT-qPCR. Dashed lines indicated a 50% reduction in viral infectivity. Data were shown as mean ± SD of representative experiments. **C.** Binding kinetics of isolated mAbs with SARS-CoV-2 RBD were measured by Surface Plasmon Resonance (SPR). The purified antibody was captured onto the CM5 sensor chip, followed by the injection of soluble SARS-CoV-2 RBD at five different concentrations. The experimental data of 58G6 and 510A5 were shown in the top and bottom figures in **C** respectively. The results presented are representatives of two independent experiments.

Figure S1. The optimization of the screening platform. A. The conventional screening of neutralizing antibodies. Antigen-specific B cells from PBMCs were sorted on day 1. The single-cell BCR genes were amplified by PCR on day 2. The antibody expression vectors were constructed in the next three days, including the PCR product sequencing, the primer synthesis, the ligation of genes and vectors, the DNA transformation and the plasmid extraction. The purified plasmids were transfected into HEK293T cells on day 5. After 48 hours, the cell supernatants were collected and analyzed with specific antigens by ELISA. Specific antibodies are used for following antibody expression and purification. Purified antibodies were screened as neutralizing candidates. **B.** The key parameters affecting screening efficiency. The following steps of the screening processes were carefully modified: multi-step sorting for the individual samples or the pooled samples, labeling S or S-RBD specific B cells, expressing antibodies using linear expression cassettes or plasmids, and designing preferred primers for the single-cell BCR cloning. To reduce time-consuming and workload, it is the critical step to screen neutralizing antibodies during the initial screening in the sixty days. Two methods for neutralization evaluation, competitive ELISA method in 3 hours or pseudovirus assay for 48 hours, were used side by side for confirmation of nAb neutralizing capability. **C.** The optimized strategy of neutralizing antibodies development. One day after PBMC thawing, specific B cell sorting was performed on day 1. A single BCR gene was cloned on day 2, using the 2nd PCR product to construct the linear expression cassettes, which were termed as the transfection targets to be introduced directly into HEK293T cells with liposome, without constructing plasmid, to shorten the screening duration. After 48 hours, the supernatants of each transfected samples were harvested and analyzed via ELISA and pseudovirus neutralization assay for evaluating specificity and neutralization.

Figure S2. The influence of dead cells on the sorting of RBD-specific memory B cells. Gating strategy to remove dead cells: SSC-A versus FSC-A selected cell populations, then FSC-A versus FSC-H excluded doublets and FSC-H versus Dead Dye removed dead cells. Memory B cells were gated by $CD19^{+}IgD^{-}IgG^{+}$ Cells (**A**), without removing dead cells in the gating strategy (**B**).

Figure S3. Schematic diagram of BCR RT-PCR and linear expression cassettes construction. A. Schema depicting workflow of the constructed linear expression cassettes. PCR amplified the variable region genes in single B cells. The BCR cDNAs was obtained from RBD-specific memory B cell by RT-PCR and the linear expression cassettes were amplified via three rounds of PCR. A primary PCR utilized gene-specific primers at both the 5′ and 3′ ends. The 5′ oligonucleotides bound the leader sequence (L). The 3′ reverse primer was connected with heavy or light constant regions. In the secondary PCR, a 5′ forward primer annealed to an "adapter", which was encoded at the 5′ end of the first PCR product, were used in combination with a 3′ reverse primer annealing to the J gene of Ab variable region. The secondary oligonucleotides provided 20 base-pair overlap regions: at the 5′ end with human cytomegalovirus (CMV) promoter fragment, and at the 3' end with a heavy or light chain constant region fragment containing a polyadenylation sequence. Then, in a tertiary PCR, the DNAs of variable region, the CMV promoter fragment, and the constant region fragments were combined and amplified to produce two separate linear expression cassettes. **B.** The amplified products from BCR cDNAs were electrophoresed and stained with ethidium bromide. **(a)** Agarose gel of variable region BCR genes. Lane "M", 2 kb DNA ladder, Lane 1-24, heavy chain variable region and Lane 25-48, light chain variable region. **(b)** Agarose gel of linear expression cassettes. Lane "M", 5 kb DNA ladder, Lane 1-24, the linear expression cassettes of heavy chains and Lane 25-48, the linear expression cassettes of light chains.

Figure S4. Usage and pairing of heavy and light chains for all specific antibodies. A. Frequencies of variable light chain gene (VL) clusters for neutralizing (activity > 75%) and potential non-neutralizing (activity < 75%) antibodies. V gene segments were ranked by frequencies of neutralizing Abs. **B.** Frequencies of various CDRL3 length of potential neutralizing and non-neutralizing antibodies. **C.** Clonal expanded heavy and light clusters were paired and highlighted in different colors.

Figure S5. Phylogenetic analysis of VH (up) and VL (down) genes for RBD-binding antibodies. Clonal expanded VH and VL clusters were paired and highlighted in various colors. The red stars represented individual neutralizing antibodies. Branch lengths were drawn to scale so that sequence relatedness could be readily assessed.

References

1. de Wit, E., van Doremalen, N., Falzarano, D. & Munster, V.J. SARS and MERS: recent insights into emerging coronaviruses. Nature Reviews Microbiology 14, 523-534 (2016).
2. Cummings, M.J., et al. Epidemiology, clinical course, and outcomes of critically ill adults with COVID-19 in New York City: a prospective cohort study. The Lancet 395, 1763-1770 (2020).
3. Chen, N., et al. Epidemiological and clinical characteristics of 99 cases of 2019 novel coronavirus pneumonia in Wuhan, China: a descriptive study. Lancet (London, England) 395, 507-513 (2020).
4. Wang, C., Horby, P.W., Hayden, F.G. & Gao, G.F. A novel coronavirus outbreak of global health concern. The Lancet 395, 470-473 (2020).
5. Mair-Jenkins, J., et al. The effectiveness of convalescent plasma and hyperimmune immunoglobulin for the treatment of severe acute respiratory infections of viral etiology: a systematic review and exploratory meta-analysis. The Journal of infectious diseases 211, 80-90 (2015).
6. Ko, J.H., et al. Challenges of convalescent plasma infusion therapy in Middle East respiratory coronavirus infection: a single centre experience. Antiviral therapy 23, 617-622 (2018).
7. Iwasaki, A. & Yang, Y. The potential danger of suboptimal antibody responses in COVID-19. Nature Reviews Immunology 20, 339-341 (2020).
8. Walls, A.C., et al. Structure, Function, and Antigenicity of the SARS-CoV-2 Spike Glycoprotein. Cell 181, 281-292.e286 (2020).
9. Hoffmann, M., et al. SARS-CoV-2 Cell Entry Depends on ACE2 and TMPRSS2 and Is Blocked by a Clinically Proven Protease Inhibitor. Cell 181, 271-280.e278 (2020).
10. Wu, Y., et al. A noncompeting pair of human neutralizing antibodies block COVID-19 virus binding to its receptor ACE2. Science 368, 1274-1278 (2020).
11. Hansen, J., et al. Studies in humanized mice and convalescent humans yield a SARS-CoV-2 antibody cocktail. Science (2020).
12. Chi, X., et al. A neutralizing human antibody binds to the N-terminal domain of the Spike protein of SARS-CoV-2. Science 369, 650-655 (2020).
13. Brouwer, P.J.M., et al. Potent neutralizing antibodies from COVID-19 patients define multiple targets of vulnerability. Science 369, 643-650 (2020).
14. Zost, S.J., et al. Potently neutralizing and protective human antibodies against SARS-CoV-2. Nature (2020).
15. Shi, R., et al. A human neutralizing antibody targets the receptor-binding site of SARS-CoV-2. Nature 584, 120-124 (2020).
16. Pinto, D., et al. Cross-neutralization of SARS-CoV-2 by a human monoclonal SARS-CoV antibody. Nature 583, 290-295 (2020).
17. Liu, L., et al. Potent neutralizing antibodies against multiple epitopes on SARS-CoV-2 spike. Nature (2020).
18. Ju, B., et al. Human neutralizing antibodies elicited by SARS-CoV-2 infection. Nature 584, 115-119 (2020).
19. Zost, S.J., et al. Rapid isolation and profiling of a diverse panel of human monoclonal antibodies targeting the SARS-CoV-2 spike protein. Nat Med (2020).
20. Wang, C., et al. A human monoclonal antibody blocking SARS-CoV-2 infection. Nat Commun 11, 2251 (2020).

21. Cao, Y., et al. Potent Neutralizing Antibodies against SARS-CoV-2 Identified by High-Throughput Single-Cell Sequencing of Convalescent Patients' B Cells. Cell 182, 73-84 e16 (2020).
22. Baum, A., et al. Antibody cocktail to SARS-CoV-2 spike protein prevents rapid mutational escape seen with individual antibodies. eabd0831 (2020).
23. Jin, A., et al. A rapid and efficient single-cell manipulation method for screening antigen-specific antibody-secreting cells from human peripheral blood. Nat Med 15, 1088-1092 (2009).
24. Akkaya, M., Kwak, K. & Pierce, S.K. B cell memory: building two walls of protection against pathogens. Nature Reviews Immunology 20, 229-238 (2020).
25. Phan, T.G. & Tangye, S.G. Memory B cells: total recall. Current opinion in immunology 45, 132-140 (2017).
26. Tiller, T., et al. Efficient generation of monoclonal antibodies from single human B cells by single cell RT-PCR and expression vector cloning. J Immunol Methods 329, 112-124 (2008).
27. Smith, K., et al. Rapid generation of fully human monoclonal antibodies specific to a vaccinating antigen. Nat Protoc 4, 372-384 (2009).
28. Liao, H.X., et al. High-throughput isolation of immunoglobulin genes from single human B cells and expression as monoclonal antibodies. J Virol Methods 158, 171-179 (2009).
29. Long, Q.-X., et al. Antibody responses to SARS-CoV-2 in patients with COVID-19. Nature Medicine 26, 845-848 (2020).
30. Briney, B., Inderbitzin, A., Joyce, C. & Burton, D.R. Commonality despite exceptional diversity in the baseline human antibody repertoire. Nature 566, 393-397 (2019).
31. Wu, N.C., et al. In vitro evolution of an influenza broadly neutralizing antibody is modulated by hemagglutinin receptor specificity. Nature Communications 8, 15371 (2017).
32. Yu, L. & Guan, Y. Immunologic Basis for Long HCDR3s in Broadly Neutralizing Antibodies Against HIV-1. Front Immunol 5, 250 (2014).
33. Jiang, S., Hillyer, C. & Du, L. Neutralizing Antibodies against SARS-CoV-2 and Other Human Coronaviruses. Trends in Immunology 41, 355-359 (2020).
34. Kreer, C., et al. Longitudinal Isolation of Potent Near-Germline SARS-CoV-2-Neutralizing Antibodies from COVID-19 Patients. Cell (2020).
35. Tian, X., et al. Potent binding of 2019 novel coronavirus spike protein by a SARS coronavirus-specific human monoclonal antibody. Emerg Microbes Infect 9, 382-385 (2020).
36. Yan, R., et al. Structural basis for the recognition of SARS-CoV-2 by full-length human ACE2. Science 367, 1444-1448 (2020).
37. Ou, X., et al. Characterization of spike glycoprotein of SARS-CoV-2 on virus entry and its immune cross-reactivity with SARS-CoV. Nature Communications 11, 1620 (2020).
38. Nie, J., et al. Establishment and validation of a pseudovirus neutralization assay for SARS-CoV-2. Emerging Microbes & Infections 9, 680-686 (2020).

Figure 1

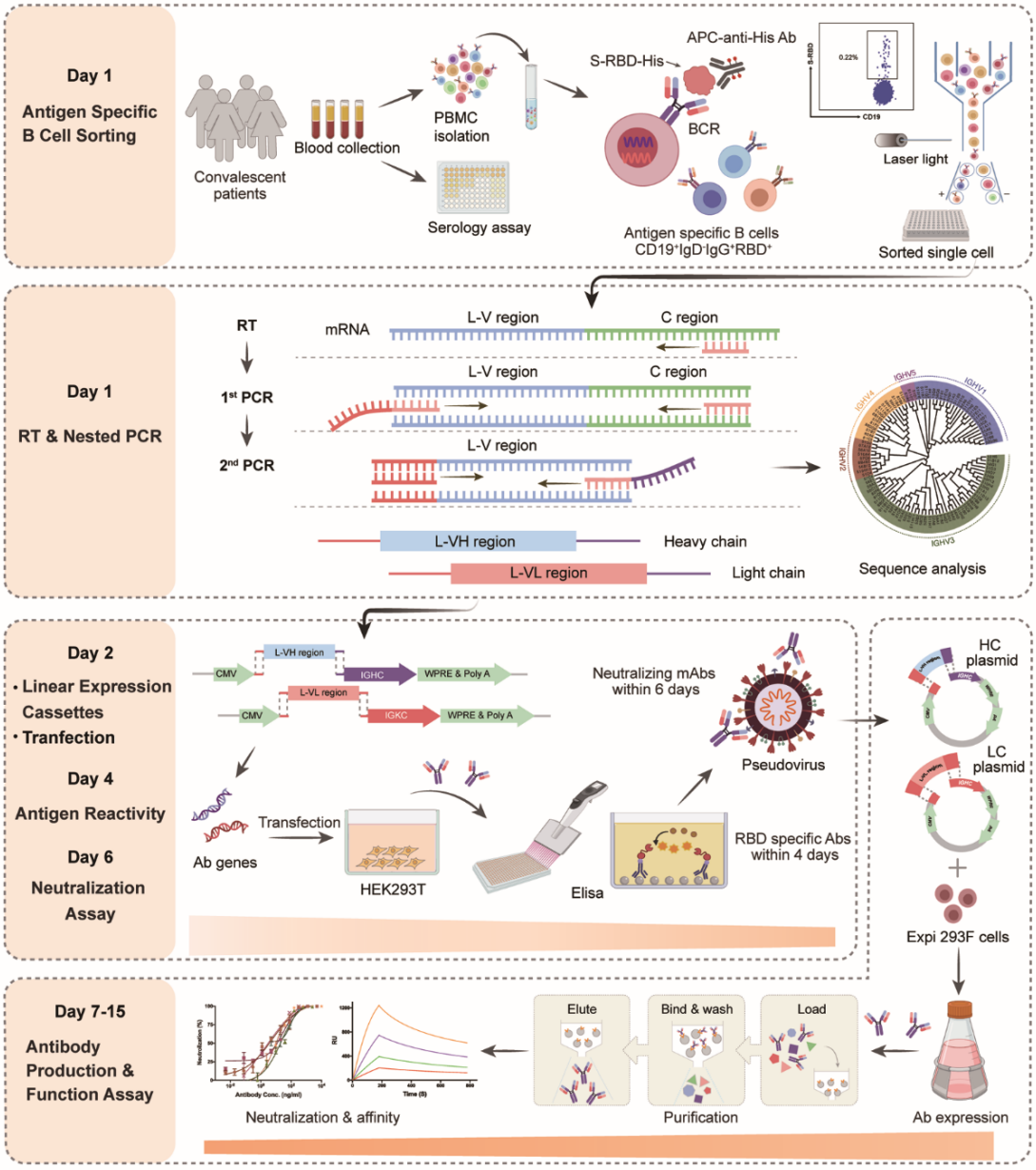

Figure 2

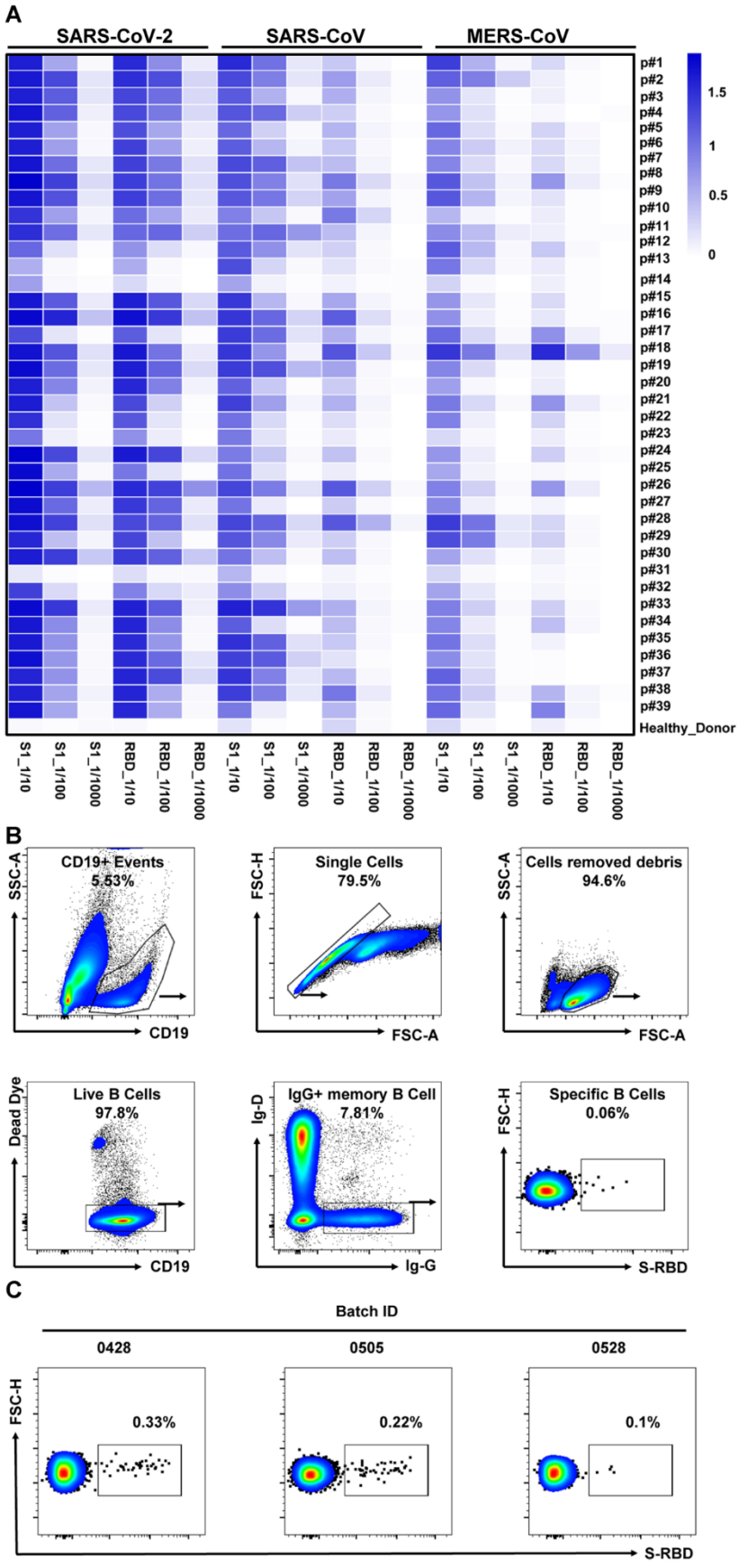

Figure 3

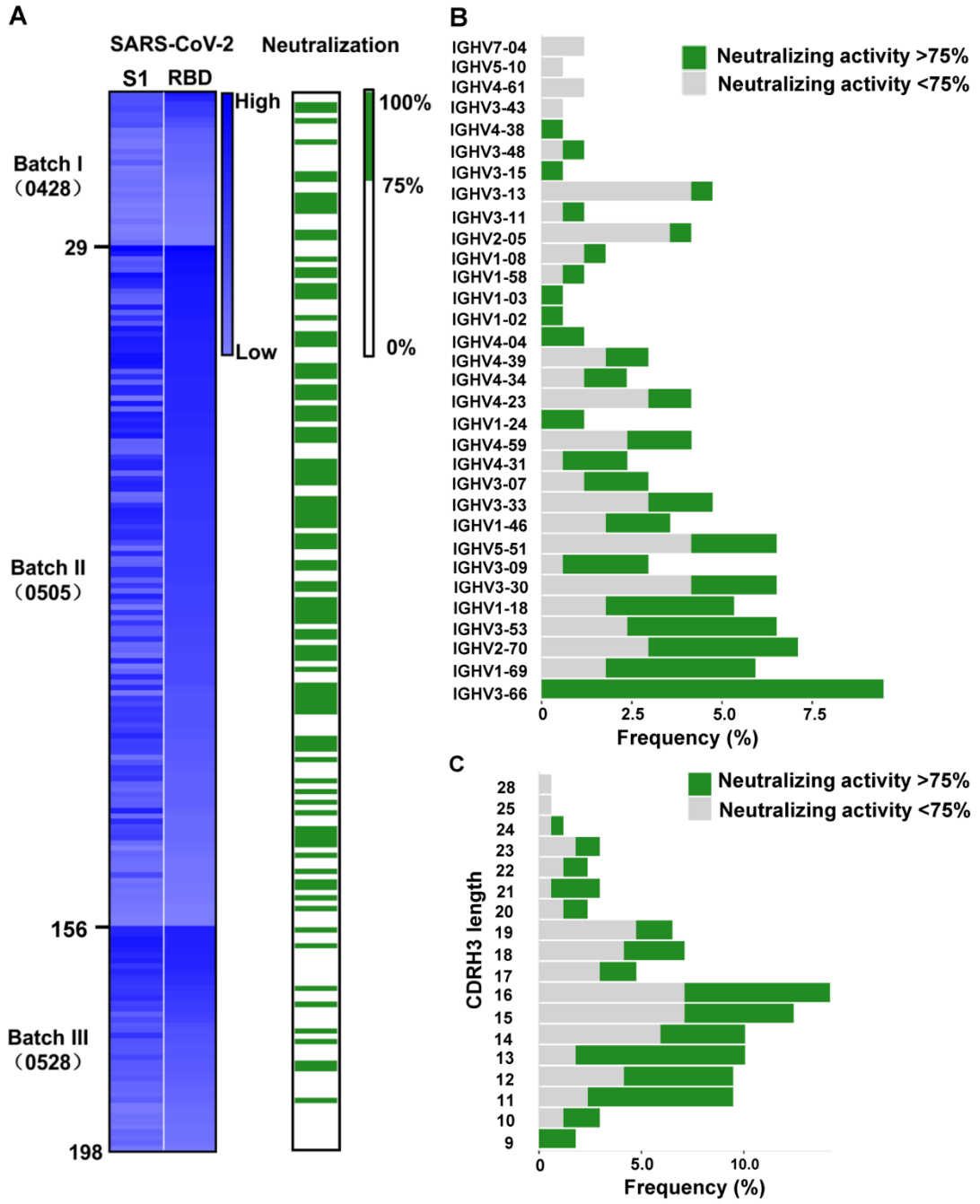

Figure 4

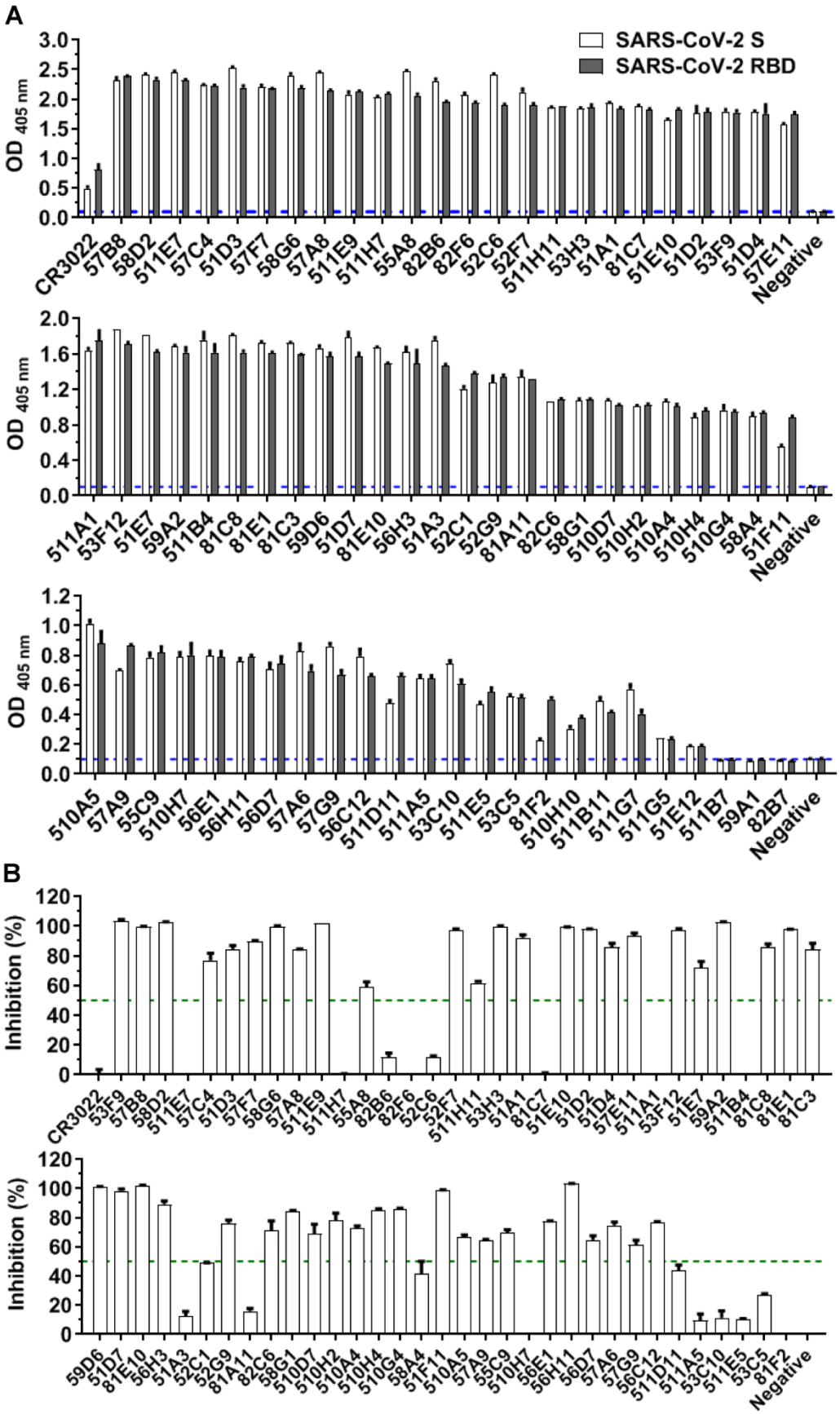

Figure 5

A

Number	mAb	Concentration (μg/ml) 18.76	9.38	4.69	2.35	1.17	0.59	0.29	0.14	Number	mAb	Concentration (μg/ml) 18.76	9.38	4.69	2.35	1.17	0.59	0.29	0.14
1	58G6	-	-	-	-	-	-	-	-	25	57A9	-	-	-	-	+	++	+++	++++
2	510A5	-	-	-	-	-	-	-	-	26	58G1	-	-	-	-	+	++	+++	++++
3	13G9*	-	-	-	-	-	-	-	-	27	510D7	-	-	-	-	+	++	+++	++++
4	510A4	-	-	-	-	-	-	-	++	28	510H4	-	-	-	-	+	++	+++	++++
5	51D3	-	-	-	-	-	-	+	++	29	52C6	-	-	-	+	+	+++	++++	++++
6	55A8	-	-	-	-	-	-	+	++	30	510H7	-	-	-	+	++	+++	++++	++++
7	51A1	-	-	-	-	-	-	+	+++	31	56E1	-	-	-	+	++	+++	++++	++++
8	81E1	-	-	-	-	-	-	+	+++	32	56H3	-	-	-	+	++	+++	++++	++++
9	51E10	-	-	-	-	-	-	+	+++	33	51F11	-	-	-	+	++	+++	++++	++++
10	51D7	-	-	-	-	-	-	+	+++	34	57C4	-	-	+	++	+++	++++	++++	++++
11	07C1	-	-	-	-	-	+	+	+++	35	07B7	-	-	+	++	+++	++++	++++	++++
12	53H3	-	-	-	-	-	+	+	+++	36	82F6	-	+	++	+++	++++	++++	++++	++++
13	52F7	-	-	-	-	-	+	+	+++	37	511G7	-	+	++	+++	++++	++++	++++	++++
14	57B8	-	-	-	-	-	+	++	+++	38	51E7	-	+	++	+++	++++	++++	++++	++++
15	57F7	-	-	-	-	-	+	++	+++	39	57A6	-	+	++	+++	++++	++++	++++	++++
16	51D4	-	-	-	-	-	+	++	+++	40	52G9	+	+	++	+++	++++	++++	++++	++++
17	55C9	-	-	-	-	-	+	++	+++	41	56C12	+	++	+++	++++	++++	++++	++++	++++
18	56D7	-	-	-	-	-	+	++	+++	42	510G4	+	+++	++++	++++	++++	++++	++++	++++
19	510H2	-	-	-	-	-	+	++	+++	43	81C8	+	+++	++++	++++	++++	++++	++++	++++
20	81C3	-	-	-	-	-	+	++	+++	44	511A5	+	+++	++++	++++	++++	++++	++++	++++
21	53F12	-	-	-	-	+	+	+++	+++	45	511B4	+	+++	++++	++++	++++	++++	++++	++++
22	82A6	-	-	-	-	+	+	++	++++	46	57A8	++	+++	++++	++++	++++	++++	++++	++++
23	51D2	-	-	-	-	+	++	+++	++++	47	57G9	++	++++	++++	++++	++++	++++	++++	++++
24	57E11	-	-	-	-	+	++	+++	++++	48	51E12	++++	++++	++++	++++	++++	++++	++++	++++

B

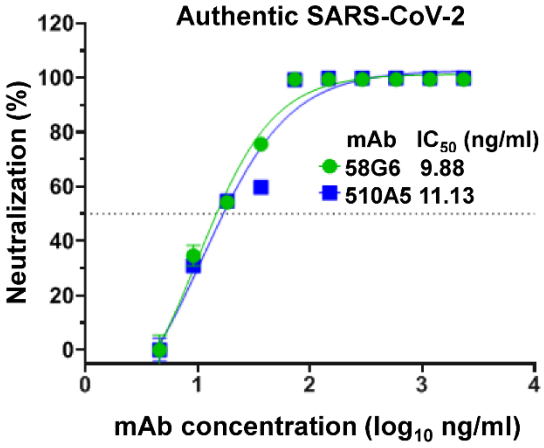

C

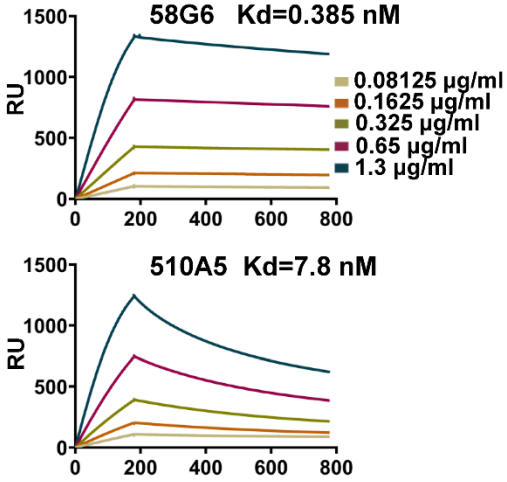

Figure S1

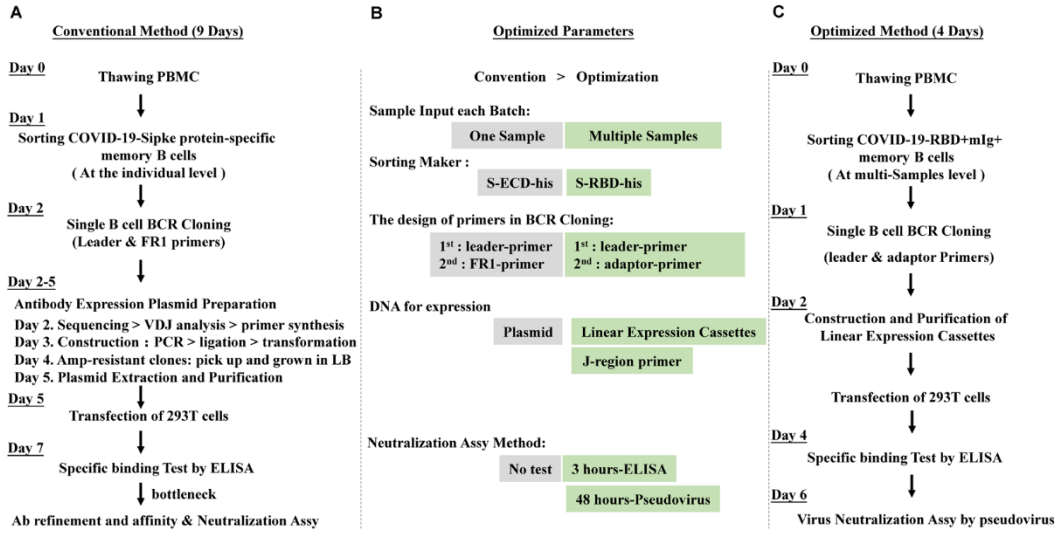

Figure S2

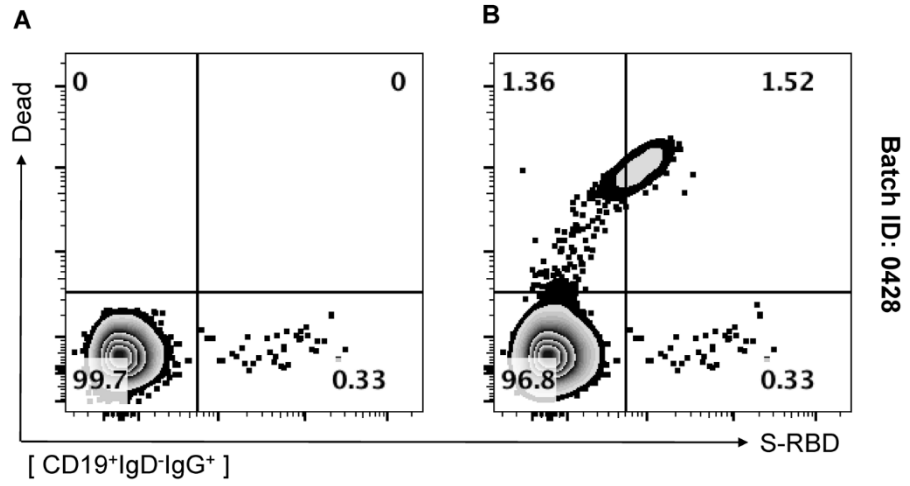

Figure S3

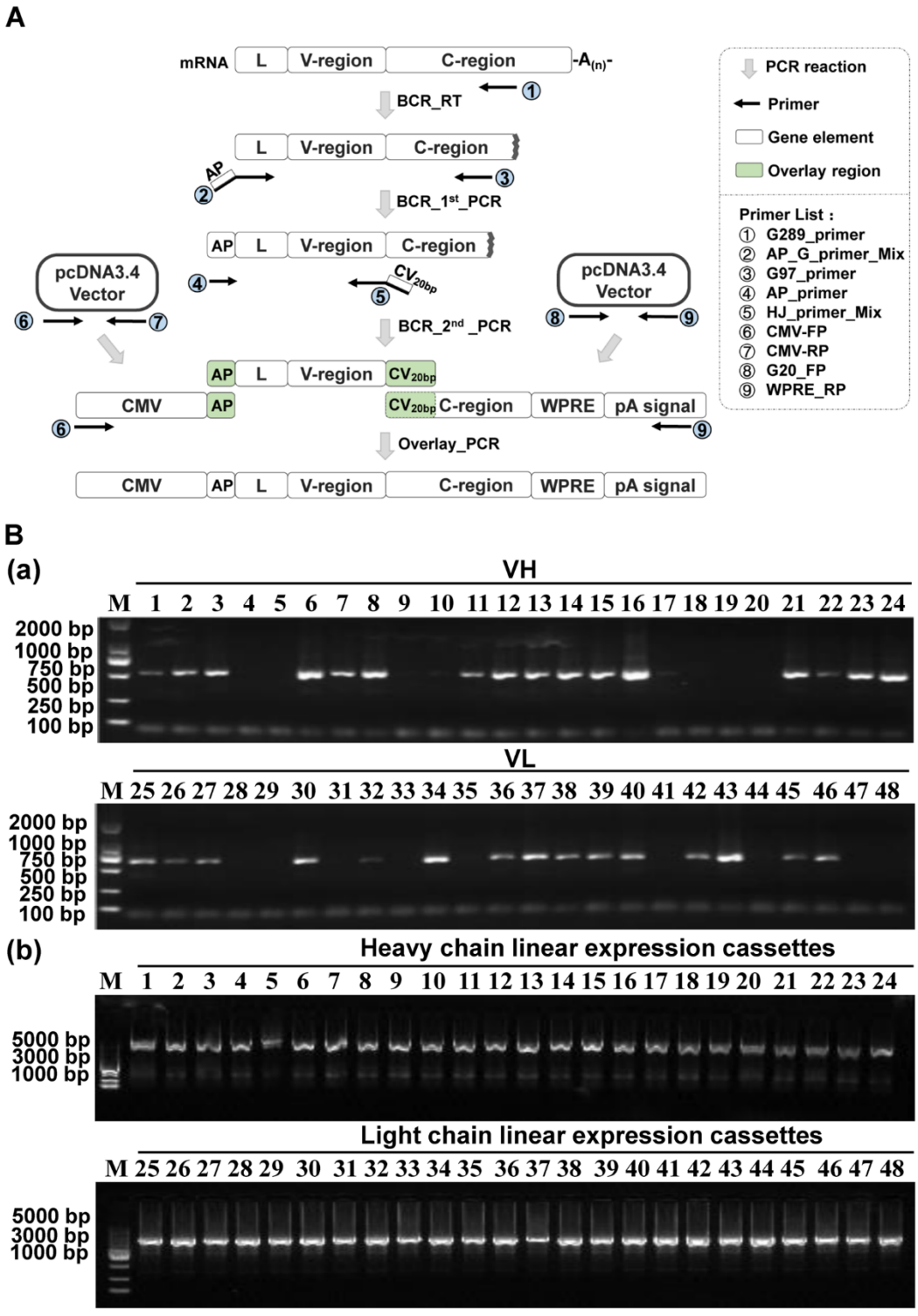

Figure S4

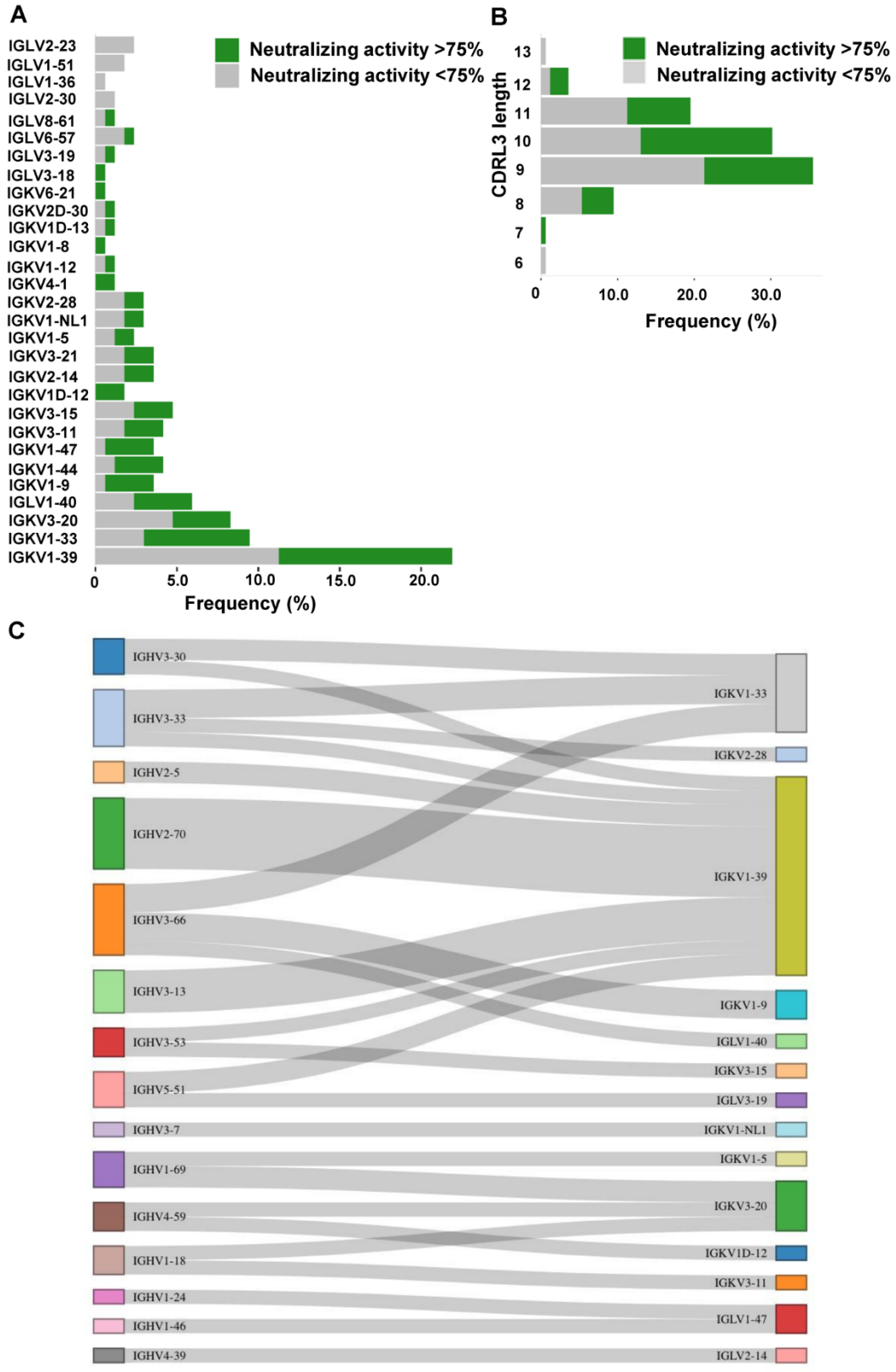

Figure S5

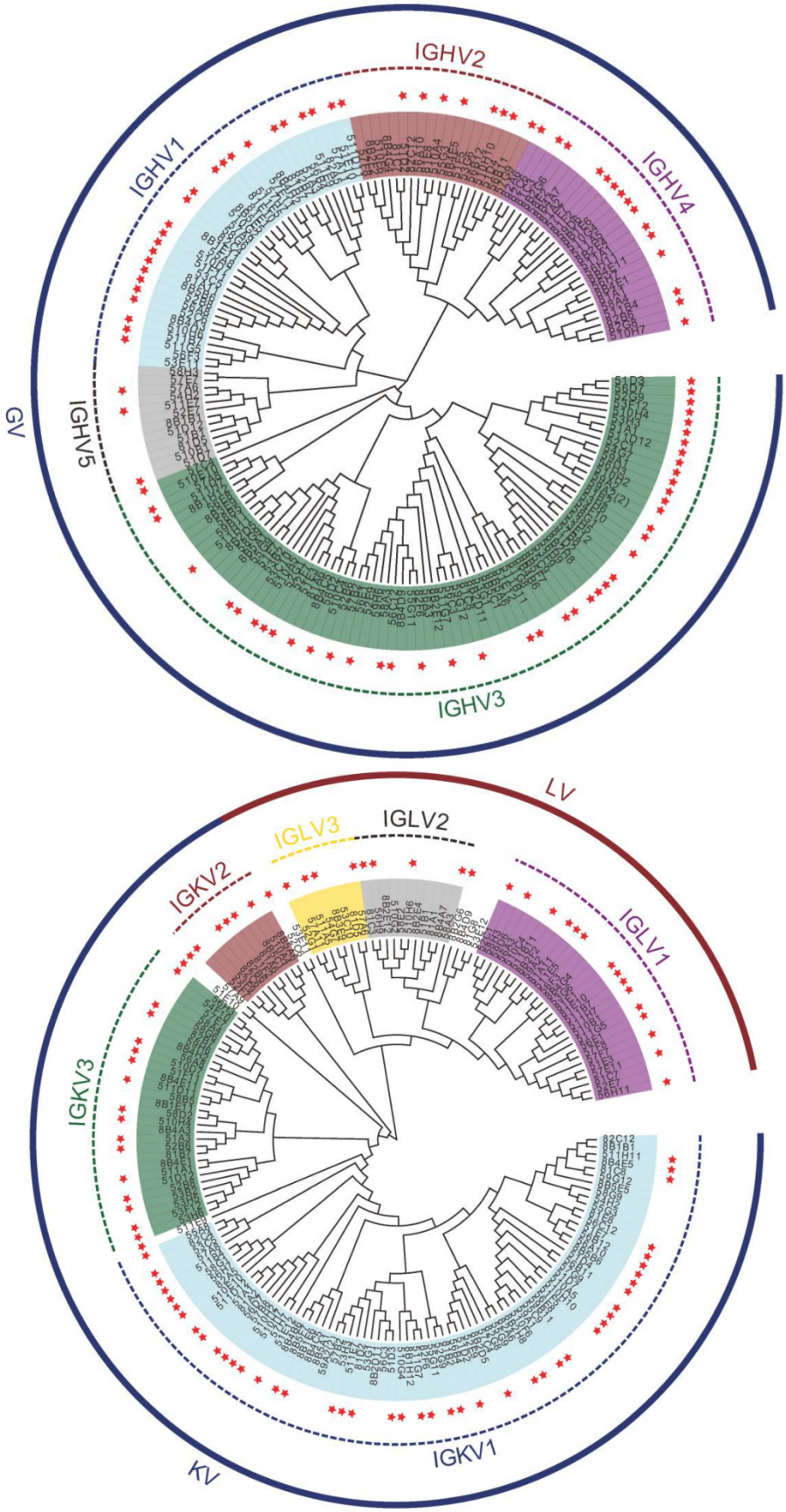

Table S1. Patient information

Subject	Age (years)	Sex	Subjsct type	Clinical classification (mild:0, severe:1)	City where infected	Date of admission	Date of discharge	Date of blood sample collection	Volume of collected blood sample
P#1	46	F	SARS-CoV-2 convalescence patient	0	Chongqing	2020/2/3	2020/2/28	2020/3/16	30ml
P#2	50	M	SARS-CoV-2 convalescence patient	0	Chongqing	2020/2/2	2020/2/28	2020/3/16	30ml
P#3	54	M	SARS-CoV-2 convalescence patient	1	Chongqing	2020/1/29	2020/2/18	2020/3/16	30ml
P#4	47	M	SARS-CoV-2 convalescence patient	1	Chongqing	2020/1/27	2020/2/23	2020/3/16	30ml
P#5	48	F	SARS-CoV-2 convalescence patient	0	Chongqing	2020/2/16	2020/2/28	2020/3/16	30ml
P#6	31	M	SARS-CoV-2 convalescence patient	0	Chongqing	2020/1/30	2020/2/10	2020/3/16	30ml
P#7	45	F	SARS-CoV-2 convalescence patient	0	Chongqing	2020/2/1	2020/2/15	2020/3/16	30ml
P#8	51	F	SARS-CoV-2 convalescence patient	0	Chongqing	2020/1/31	2020/2/17	2020/3/16	50ml
P#9	48	M	SARS-CoV-2 convalescence patient	1	Chongqing	2020/1/30	2020/2/18	2020/4/1	50ml
P#10	31	M	SARS-CoV-2 convalescence patient	0	Chongqing	2020/1/29	2020/2/18	2020/4/1	50ml
P#11	54	M	SARS-CoV-2 convalescence patient	0	Chongqing	2020/2/2	2020/2/18	2020/4/1	30ml
P#12	47	F	SARS-CoV-2 convalescence patient	0	Chongqing	2020/1/31	2020/2/10	2020/4/1	10ml
P#13	38	M	SARS-CoV-2 convalescence patient	0	Chongqing	2020/2/10	2020/2/19	2020/4/1	10ml
P#14	33	F	SARS-CoV-2 convalescence patient	0	Chongqing	2020/2/10	2020/3/9	2020/4/1	10ml
P#15	44	M	SARS-CoV-2 convalescence patient	0	Chongqing	2020/2/5	2020/2/14	2020/4/1	50ml
P#16	60	F	SARS-CoV-2 convalescence patient	0	Chongqing	2020/2/11	2020/3/5	2020/4/1	30ml
P#17	48	M	SARS-CoV-2 convalescence patient	0	Chongqing	2020/2/12	2020/3/6	2020/4/1	30ml
P#18	53	F	SARS-CoV-2 convalescence patient	0	Chongqing	2020/2/16	2020/2/28	2020/4/1	10ml
P#19	57	M	SARS-CoV-2 convalescence patient	0	Chongqing	2020/1/29	2020/2/14	2020/4/1	10ml
P#20	44	M	SARS-CoV-2 convalescence patient	0	Chongqing	2020/2/6	2020/2/29	2020/4/1	10ml
P#21	44	F	SARS-CoV-2 convalescence patient	0	Chongqing	2020/2/13	2020/3/11	2020/4/1	30ml
P#22	20	F	SARS-CoV-2 convalescence patient	0	Chongqing	2020/2/15	2020/2/25	2020/4/1	30ml
P#23	37	M	SARS-CoV-2 convalescence patient	0	Chongqing	2020/2/2	2020/3/9	2020/4/1	50ml
P#24	44	F	SARS-CoV-2 convalescence patient	0	Chongqing	2020/2/3	2020/2/28	2020/4/1	50ml
P#25	41	M	SARS-CoV-2 convalescence patient	0	Chongqing	2020/1/31	2020/2/16	2020/4/1	14ml
P#26	66	M	SARS-CoV-2 convalescence patient	0	Chongqing	2020/2/3	2020/2/16	2020/4/1	10ml
P#27	67	F	SARS-CoV-2 convalescence patient	0	Chongqing	2020/2/4	2020/2/16	2020/4/1	10ml
P#28	50	M	SARS-CoV-2 convalescence patient	1	Chongqing	2020/2/1	2020/2/29	2020/4/1	30ml
P#29	50	F	SARS-CoV-2 convalescence patient	0	Chongqing	2020/1/28	2020/2/29	2020/4/1	50ml
P#30	49	F	SARS-CoV-2 convalescence patient	0	Chongqing	2020/2/8	2020/3/6	2020/4/1	30ml
P#31	56	M	SARS-CoV-2 convalescence patient	0	Chongqing	2020/2/1	2020/2/9	2020/4/1	30ml
P#32	55	M	SARS-CoV-2 convalescence patient	0	Chongqing	2020/2/14	2020/2/21	2020/4/1	50ml
P#33	45	F	SARS-CoV-2 convalescence patient	0	Chongqing	2020/2/1	2020/2/15	2020/4/1	30ml
P#34	47	F	SARS-CoV-2 convalescence patient	0	Chongqing	2020/2/6	2020/2/17	2020/4/1	10ml
P#35	34	M	SARS-CoV-2 convalescence patient	0	Chongqing	2020/1/28	2020/2/7	2020/4/1	10ml
P#36	47	M	SARS-CoV-2 convalescence patient	1	Chongqing	2020/1/27	2020/2/23	2020/4/1	50ml
P#37	56	M	SARS-CoV-2 convalescence patient	0	Chongqing	2020/1/30	2020/2/7	2020/4/1	40ml
P#38	63	F	SARS-CoV-2 convalescence patient	0	Chongqing	2020/2/1	2020/2/25	2020/4/1	10ml
P#39	37	M	SARS-CoV-2 convalescence patient	0	Chongqing	2020/1/27	2020/2/14	2020/4/1	10ml

Table S2. Three batches of S-RBD specific B memory cell sorting

Batch	Sample count	Subject	Volume of blood used for sorting(ml)	Total volume of blood(ml)	Number of sorted 96 wells plates	Number of Paired mAbs after BCR RT-PCR	Number of Specific mAbs (note-01)	Number of Neutralizing mAbs (note-01)
0428	1	p#10	10	70	2	72	29	12
	2	p#11	10					
	3	p#29	10					
	4	p#30	10					
	5	p#32	10					
	6	p#36	10					
	7	p#37	10					
0505	1	p#8	10	60	11	324	127	75
	2	p#16	15					
	3	p#17	15					
	4	p#26	10					
	5	p#27	10					
0528	1	p#01	10	75	4.5	101	42	9
	2	p#03	10					
	3	p#04	10					
	4	p#06	10					
	5	p#09	10					
	6	p#22	10					
	7	p#25	5					
	8	p#28	5					
	9	p#31	5					
					Sum:	497	198	96

Note-01: the linear expression cassettes were transfected into 293T cells for expressing Ab proteins. The supernatants of cell cultures were collected 48hs later. the specific binding ability were assessed by ELISA. the neutralizaiton capability were assessed by pseudovirus assay.

Table S3. BCR RT-PCR Reaction mixture and PCR Program setup

Section 01. Single Cell BCR RT-PCR Procedure

1. Preparation of PCR Reaction Mixture

(1) Preparation of RT

a. Preparation of RT_Mix_A (5μl/tube)

Seq.	Component	Amount (μl)
1	Water	2.6
2	2.5 mM dNTPs	2
3	BCR_RT_Primer_Mix	0.4

b. Preparation of RT_Mix_B (5μl/tube)

Seq.	Component	Amount (μl)
4	Water	2.25
5	5×PrimeScript II Buffer	2
6	200 U/μl PrimeScript II Reverse Transcriptase	0.5
7	40,000 U/ml RNase Inhibitor, Murine (NEB)	0.25

(2) Preparation of 1st and 2nd PCR (10μl/tube)

1st_PCR_Mix_N and 2nd_PCR_Mix_N use the same reaction condition except the primers.

Seq.	Component	Amount (μl)
1	2×PrimeSTAR GC Buffer (Takara)	5
2	nuclease-free water	2.75
3	2.5 mM dNTP	0.8
4	10 μM Forward Primer	0.2
5	10 μM Reverse Primer	0.2
6	2.5 U/μl PrimeSTAR HS DNA polymerase	0.05
7	Template	0

(3) Usage of primers

a. For 1st_PCR_Mix

	For 1st_PCR_Mix_Gamma	For 1st_PCR_Mix_Kappa	For 1st_PCR_Mix_Lambda
Forward Primer	AP_G_leader Mix	AP_K_leader Mix	AP_L_leader Mix
Reverse Primer	G289_primer(10μM)	K244_Primer(10μM)	L81_Primer(10μM)

b. For 2nd_PCR_Mix

	For 2nd _PCR_Mix_Gamma	For 2nd _PCR_Mix_Kappa	For 2nd _PCR_Mix_Lambda
Forward Primer	10 μM AP_Primer	10 μM AP_Primer	10 μM AP_Primer
Reverse Primer	IGHJ_region_Primer Mix	10 μM K194_Primer Mix	10 μM L19_Primer Mix

2. Operation Procedure

(1) Take out the sorted 96-well plate at -80. Add 5μl RT_Mix_A to each well, and rinse the well to promote cell RNA dissolution.

(2) Incubate the plate at 65° for 5min and put it on ice immediately.

(3) Add 5μl of RT_Mix_B to each well of the plate, mix and centrifuge, and then perform RT reaction.

(4) 9μl aliquots of 1st_PCR_Mix in a new 96 wells plate, add 1μl RT product to each well, and then perform 1st PCR Reaction.

(5) After PCR is completed, the 1st product is ten-fold diluted, and 1μl is used as a template for the next round of PCR.

(6) 9μl aliquot 2nd_PCR_Mix in a new 96 wells plate, add 1μl 1st diluted product to each well, and then perform 2nd PCR Reaction.

(7) Prepare 2% agar gel, load 3μl sample to analysis PCR resμlt.

Section 02. PCR Program Setup

1. For RT Reaction

45°	45min
70°	15min
4°	infinity

2. For 1st PCR Reaction

95	3min	
95	10s	30cycles
55	5s	
72°	1min	
72°	5min	
4°	infinity	

3. For 2nd PCR Reaction

95	3min	
95	10s	35cycles
55	5s	
72°	45s	
72°	5min	
4°	infinity	

Table S4. Primers List of BCR RT-PCR

Primer_Name	V/D/J gene segments	Primer_Sequence(5`>3`)	Usage description
GV_01	IGHV1-18*01	CGGTACCGCGGGCCCGGGAatggactggacctggagcat	AP_G_Leader_Mix
GV_02	IGHV1-2*01	CGGTACCGCGGGCCCGGGAatggactggacctggaggat	As forward primer of heavy chain 1st PCR
GV_03	IGHV1-24*01	CGGTACCGCGGGCCCGGGAatggactgcacctggaggat	
GV_04	IGHV1-38-4*01	CGGTACCGCGGGCCCGGGAatggactggaactggaggat	
GV_05	IGHV1-45*01	CGGTACCGCGGGCCCGGGAatggactggacctggagaat	
GV_06	IGHV1-46*01	CGGTACCGCGGGCCCGGGAatggactggacctggagggt	
GV_07	IGHV1-58*01	CGGTACCGCGGGCCCGGGAatggactggatttggaggat	
GV_08	IGHV1-69*01	CGGTACCGCGGGCCCGGGAatggactggacctggaggtt	
GV_09	IGHV2-26*01	CGGTACCGCGGGCCCGGGAatggacacactttgctacac	
GV_10	IGHV2-5*01	CGGTACCGCGGGCCCGGGAatggacacactttgctccac	
GV_11	IGHV2-70*01	CGGTACCGCGGGCCCGGGAatggacatactttgttccac	
GV_12	IGHV2/OR16-5*01	CGGTACCGCGGGCCCGGGAatggacacgttttgctccac	
GV_13	IGHV3-11*01	CGGTACCGCGGGCCCGGGAatggagtttgggctgagctg	
GV_14	IGHV3-13*01	CGGTACCGCGGGCCCGGGAatggagttggggctgagctg	
GV_15	IGHV3-16*01	CGGTACCGCGGGCCCGGGAatggaatttgggctgagctg	
GV_16	IGHV3-21*01	CGGTACCGCGGGCCCGGGAatggaactggggctccgctg	
GV_17	IGHV3-43*01	CGGTACCGCGGGCCCGGGAatggagtttggactgagctg	
GV_18	IGHV3-48*01	CGGTACCGCGGGCCCGGGAatggagttggggctgtgctg	
GV_19	IGHV3-49*01	CGGTACCGCGGGCCCGGGAatggagtttgggcttagctg	
GV_20	IGHV3-53*01	CGGTACCGCGGGCCCGGGAatggagttttggctgagctg	
GV_21	IGHV3-64*01	CGGTACCGCGGGCCCGGGAatgacggagtttgggctgag	
GV_22	IGHV3-64D*06	CGGTACCGCGGGCCCGGGAatggagttctggctgagctg	
GV_23	IGHV3-7*01	CGGTACCGCGGGCCCGGGAatggaattggggctgagctg	
GV_24	IGHV3-9*01	CGGTACCGCGGGCCCGGGAatggagttgggactgagctg	
GV_25	IGHV4-28*01	CGGTACCGCGGGCCCGGGAatgaaacacctgtggttctt	
GV_26	IGHV4-38-2*02	CGGTACCGCGGGCCCGGGAatgaagcacctgtggttttt	
GV_27	IGHV4-39*01	CGGTACCGCGGGCCCGGGAatgaagcacctgtggttctt	
GV_28	IGHV4-59*01	CGGTACCGCGGGCCCGGGAatgaaacatctgtggttctt	
GV_29	IGHV5-10-1*02	CGGTACCGCGGGCCCGGGAatgcaagtgggggcctctcc	
GV_30	IGHV5-51*01	CGGTACCGCGGGCCCGGGAatggggtcaaccgccatcct	
GV_31	IGHV6-1*01	CGGTACCGCGGGCCCGGGAatgtctgttctccttcctcat	
KV_01	IGKV1/OR2-0*01	CGGTACCGCGGGCCCGGGAatgagggccccactcagct	AP_K_Leader_Mix
KV_02	IGKV1/OR2-108*01	CGGTACCGCGGGCCCGGGAatggaaatgagggtccccgc	As forward primer of kappa light chain 1st PCR
KV_03	IGKV1-16*01	CGGTACCGCGGGCCCGGGAatggacatgagagtcctcgc	
KV_04	IGKV1-27*01	CGGTACCGCGGGCCCGGGAatggacatgagggtccctgc	
KV_05	IGKV1-5*01	CGGTACCGCGGGCCCGGGAatggacatgagggtccccgc	
KV_06	IGKV1-8*01	CGGTACCGCGGGCCCGGGAatgagggtccccgctcagct	
KV_07	IGKV1D-16*01	CGGTACCGCGGGCCCGGGAatggacatgagggtcctcgc	
KV_08	IGKV1D-43*01	CGGTACCGCGGGCCCGGGAatggacatgagggtgcccgc	
KV_09	IGKV2-24*01	CGGTACCGCGGGCCCGGGAatgaggctccttgctcagct	
KV_10	IGKV2-28*01	CGGTACCGCGGGCCCGGGAatgaggctccctgctcagct	
KV_11	IGKV3/OR2-268*01	CGGTACCGCGGGCCCGGGAatggaagccccagcacagct	
KV_12	IGKV3-15*01	CGGTACCGCGGGCCCGGGAatggaagccccagcgcagct	
KV_13	IGKV3-20*01	CGGTACCGCGGGCCCGGGAatggaaaccccagcgcagct	
KV_14	IGKV3-7*01	CGGTACCGCGGGCCCGGGAatggaagccccagctcagct	
KV_15	IGKV3D-7*01	CGGTACCGCGGGCCCGGGAatggaaccatggaagccccа	
KV_16	IGKV4-1*01	CGGTACCGCGGGCCCGGGAatggtgttgcagacccaggt	
KV_17	IGKV5-2*01	CGGTACCGCGGGCCCGGGAatggggtcccaggttcacct	
KV_18	IGKV6-21*01	CGGTACCGCGGGCCCGGGAatgttgccatcacaactcat	
KV_19	IGKV6D-41*01	CGGTACCGCGGGCCCGGGAatggtgtccccgttgcaatt	
LV_01	IGLV1-40*01	CGGTACCGCGGGCCCGGGAatggcctggtctcctctcct	AP_L_Leader_Mix
LV_02	IGLV1-41*01	CGGTACCGCGGGCCCGGGAatgacctgctcccctctcct	As forward primer of lambda light chain 1st PCR
LV_03	IGLV1-47*02	CGGTACCGCGGGCCCGGGAatggccggcttcctctcct	
LV_04	IGLV10-54*02	CGGTACCGCGGGCCCGGGAatgccctgggctctgctcct	
LV_05	IGLV11-55*01	CGGTACCGCGGGCCCGGGAatggccctgactcctctcct	
LV_06	IGLV2-8*02	CGGTACCGCGGGCCCGGGAatggcctgggctctgctgct	
LV_07	IGLV3-1*01	CGGTACCGCGGGCCCGGGAatggcatggatccctctctt	
LV_08	IGLV3-10*02	CGGTACCGCGGGCCCGGGAatggcctggaccctctcct	
LV_09	IGLV3-19*01	CGGTACCGCGGGCCCGGGAatggcctggacccctctctg	
LV_10	IGLV3-21*01	CGGTACCGCGGGCCCGGGAatggcctggaccgtttctcct	
LV_11	IGLV3-25*02	CGGTACCGCGGGCCCGGGAatggcctggatccctctact	
LV_12	IGLV3-27*01	CGGTACCGCGGGCCCGGGAatggcctggatccctctcct	
LV_13	IGLV3-9*02	CGGTACCGCGGGCCCGGGAatggcctggaccgctctcct	
LV_14	IGLV4-3*01	CGGTACCGCGGGCCCGGGAatggcctgggtctccttcta	
LV_15	IGLV4-60*02	CGGTACCGCGGGCCCGGGAatggcctggaccccactcct	
LV_16	IGLV5-39*02	CGGTACCGCGGGCCCGGGAatggcctggactcctctcct	
LV_17	IGLV6-57*02	CGGTACCGCGGGCCCGGGAatggcctgggctccactact	
LV_18	IGLV7-43*01	CGGTACCGCGGGCCCGGGAatggcctggactcctctctt	
LV_19	IGLV8-61*02	CGGTACCGCGGGCCCGGGAatggcctggatgatgcttct	
LV_20	IGLV8/OR8-1*02	CGGTACCGCGGGCCCGGGAatggcctgcatgatgcttct	
LV_21	IGLV9-49*02	CGGTACCGCGGGCCCGGGAatggcctgggctcctctgct	
IGHJ_01	IGHJ1*01	GATGGGCCCTTGGTGGAGGGTGAGGAGACGGTGACCAGGG	IGHJ_region_Primer_Mix
IGHJ_02	IGHJ2*01	GATGGGCCCTTGGTGGAGGGTGAGGAGACAGTGACCAGGG	
IGHJ_03	IGHJ3*01	GATGGGCCCTTGGTGGAGGGTGAAGAGACGGTGACCATTG	
IGHJ_04	IGHJ6*01	GATGGGCCCTTGGTGGAGGGTGAGGAGACGGTGACCGTGG	
IGKJ_01	IGKJ1*01	GATGGTGCAGCCACAGTTCGTTTGATTTCCACCTTGGTCC	IGKJ_region_Primer_Mix
IGKJ_02	IGKJ2*01	GATGGTGCAGCCACAGTTCGTTTGATCTCCAGCTTGGTCC	
IGKJ_03	IGKJ3*01	GATGGTGCAGCCACAGTTCGTTTGATATCCACTTTGGTCC	
IGKJ_04	IGKJ4*01	GATGGTGCAGCCACAGTTCGTTTGATCTCCACCTTGGTCC	
IGKJ_05	IGKJ5*01	GATGGTGCAGCCACAGTTCGTTTAATCTCCAGTCGTGTCC	
IGLJ_01	IGLJ1*01	GGGGCAGCCTTGGGCTGACCTAGGACGGTGACCTTGGTCC	IGLJ_region_Primer_Mix
IGLJ_02	IGLJ2*01	GGGGCAGCCTTGGGCTGACCTAGGACGGTCAGCTTGGTCC	
IGLJ_03	IGLJ4*01	GGGGCAGCCTTGGGCTGACCTAAAATGATCAGCTGGGTTC	
IGLJ_04	IGLJ5*01	GGGGCAGCCTTGGGCTGACCTAGGACGGTCAGCTCGGTCC	
IGLJ_05	IGLJ5*02	GGGGCAGCCTTGGGCTGACCTAGGACGGTCAGCTCCGTCC	
IGLJ_06	IGLJ6*01	GGGGCAGCCTTGGGCTGACCGAGGACGGTCACCTTGGTGC	
IGLJ_07	IGLJ7*01	GGGGCAGCCTTGGGCTGACCGAGGACGGTCAGCTGGGTGC	
IGLJ_08	IGLJ7*02	GGGGCAGCCTTGGGCTGACCGAGGGCGGTCAGCTGGGTGC	
G289-primer	N.D.	TCTTGTCCACCTTGGTGTTGCT	As reverse primer of heavy chain RT & 1st PCR
G97-primer	N.D.	AGTAGTCCTTGACCAGGCAGCCCAG	As reverse primer of heavy chain 2nd PCR
K244-primer	N.D.	GTTTCTCGTAGTCTGCTTTGCTCA	As reverse primer of kappa light chain RT & 1st PCR
K194-primer-01	N.D.	GTGCTGTCCTTGCTGTCCTGCT	As reverse primer of kappa light chain 2nd PCR
K194-primer-02	N.D.	GTGCTGTCCTTGCTCTCCTGCT	
L81-primer	N.D.	CACCAGTGTGGCCTTGTTGGCTTG	As reverse primer of lambda light chain RT & 1st PCR
L19-primer-01	N.D.	GGGCGGGAACAGAGTGACC	As reverse primer of lambda light chain 2nd PCR
L19-primer-02	N.D.	GGGCGGGAACAGAGTGACA	
L19-primer-03	N.D.	GGGTGGGAACAGAGTGACC	
AP3	N.D.	CGGTACCGCGGGCCCGGGA	As forward primer of 2nd PCR
G20FP	N.D.	CCCTCCACCAAGGGCCCATC	Construction of the linear antibody expression cassettes
K20FP	N.D.	CGAACTGTGGCTGCACCATC	
L20FP	N.D.	GGTCAGCCCAAGGCTGCCCC	
CMV-FP-01	N.D.	AGATATACGCGTTGACATTG	
CMV-RP	N.D.	TCCCGGGCCCGCGGTACCG	
WPRE-RP	N.D.	AGCCCCAGCTGCGCAGATCT	

Table S5. Preparation of BCR Cloning primers

Step 01. Dissolve primer powder in water
the leader primers and J-region primers are dissolved to 100uM the other primers are dissolved to 10μM
Step 02. Preparation of BCR_RT_Primer_Mix (each 2μM)
take 100μl G289_primer(10μM), K244_primer(10μM), L81 primer(10μM), respectively, then mix according to 1:1:1.
Step 03. Preparation of AP_Leader_Mix (each 2μM)
(1) For AP_G_Leader_Mix: Add 380μl water to a 1.5ml centrifuge tube, and take 20μl each of the 31 GV_N primers, and the final volume is 1000μl; (2) For AP_K_Leader_Mix: Add 620μl water to a 1.5ml centrifuge tube, and take 20μl each of the 19 KV_N primers, and the final volume is 1000μl; (3) For AP_L_Leader_Mix: Add 580μl water to a 1.5ml centrifuge tube, and take 20μl each of the 21 LV_N primers, and the final volume is 1000μl;
Step 04. Preparation of IGHJ_region_Primer_Mix (each 2μM)
Add 920μl water to a 1.5ml centrifuge tube, and take 20μl each of the 4 IGHJ_N primers, and the
Step 05. Preparation of K194_Primer_Mix
take 100μl each of the following 2 primers, then mix: K194-primer-01 (10μM) K194-primer-02 (10μM)
Step 06. Preparation of L19_Primer_Mix
take 100μl each of the following 3 primers, then mix: L19-primer-01 (10μM) L19-primer-02 (10μM) L19-primer-03 (10μM)

Table S6. Annotation of linear antibody expression cassettes

Linear expression cassettes For IGHC

CMV-FP_Primer	[AGATATACGCGTTGACATTG] [ATTATTGACTAGTTATTAATAGTAATCAATTACGGGGTCATTAGTTCATAGCCCATATATGGAGTTCCGCGTTACATAACTTACGGTAAATGGCCCGCCTGGCTGACCGCCCAACGACCCCCGCCC
CMV promoter	ATTGACGTCAATAATGACGTATGTTCCCATAGTAACGCCAATAGGGACTTTCCATTGACGTCAATGGGTGGAGTATTTACGGTAAACTGCCCACTTGGCAGTACATCAAGTGTATCATATGCCAAGTACGCCCCCTATTGACGTCAATG
CMV-RP_Primer	ACGGTAAATGGCCCGCCTGGCATTATGCCCAGTACATGACCTTATGGGACTTTCCTACTTGGCAGTACATCTACGTATTAGTCATCGCTATTACCATGGTGATGCGGTTTTGGCAGTACATCAATGGGCGTGGATAGCGGTTTGACTCA
G20_Primer	CGGGGATTTCCAAGTCTCCACCCCATTGACGTCAATGGGAGTTTGTTTTGGCACCAAAATCAACGGGACTTTCCAAAATGTCGTAACAACTCCGCCCCATTGACGCAAATGGGCGGTAGGCGTGTACGGTGGGAGGTCTATATAAGCAG
hman IGHG1 Constant region	AGCTCGTTTAGTGAACCGTCAGATCGCCTGGAGACGCCATCCACGCTGTTTTGACCTCCA] TAGAAGACACCGGGACCGATCCAGCCTCCGGACTCTAGACTTCGAATTCTGCAGTCGA [CGGTACCGCGGGCCCGGGA] [2nd-PCR
WPRE	product] [CCCTCCACCAAGGGCCCATC] [GGTCTTCCCCCTGGCACCCTCCTCCAAGAGCACCTCTGGGGGCACAGCGGCCCTGGGCTGCCTGGTCAAGGACTACTTCCCCGAACCGGTGACGGTGTCGTGGAACTCAGGCGCCCTG
poly(A) signal	ACCAGCGGCGTGCACACCTTCCCGGCTGTCCTACAGTCCTCAGGACTCTACTCCCTCAGCAGCGTGGTGACCGTGCCCTCCAGCAGCTTGGGCACCCAGACCTACATCTGCAACGTGAATCACAAGCCCAGCAACACCAAGGTGGACAA
WPRE_RP_Primer	GAAAGTTGAGCCCAAATCTTGTGACAAAACTCACACATGCCCACCGTGCCCAGCACCTGAACTCCTGGGGGGACCGTCAGTCTTCCTCTTCCCCCCAAAACCCAAGGACACCCTCATGATCTCCCGGACCCCTGAGGTCACATGCGTGG
	TGGTGGACGTGAGCCACGAAGACCCTGAGGTCAAGTTCAACTGGTACGTGGACGGCGTGGAGGTGCATAATGCCAAGACAAAGCCGCGGGAGGAGCAGTACAACAGCACGTACCGTGTGGTCAGCGTCCTCACCGTCCTGCACCAGGAC
	TGGCTGAATGGCAAGGAGTACAAGTGCAAGGTCTCCAACAAAGCCCTCCCAGCCCCCATCGAGAAAACCATCTCCAAAGCCAAAGGGCAGCCCCGAGAACCACAGGTGTACACCCTGCCCCCATCCCGGGATGAGCTGACCAAGAACCA
	GGTCAGCCTGACCTGCCTGGTCAAAGGCTTCTATCCCAGCGACATCGCCGTGGAGTGGGAGAGCAATGGGCAGCCGGAGAACAACTACAAGACCACGCCTCCCGTGCTGGACTCCGACGGCTCCTTCTTCCTCTACAGCAAGCTCACCG
	TGGACAAGAGCAGGTGGCAGCAGGGGAACGTCTTCTCATGCTCCGTGATGCATGAGGCTCTGCACAACCACTACACGCAGAAGAGCCTCTCCCTGTCTCCGGGTAAATGA] GAATTCGCGGCCGCGAGTTTGATATCT [CGACAATCAA
	CCTCTGGATTACAAAATTTGTGAAAGATTGACTGGTATTCTTAACTATGTTGCTCCTTTTACGCTATGTGGATACGCTGCTTTAATGCCTTTGTATCATGCTATTGCTTCCCGTATGGCTTTCATTTTCTCCTCCTTGTATAAATCCTG
	GTTGCTGTCTCTTTATGAGGAGTTGTGGCCCGTTGTCAGGCAACGTGGCGTGGTGTGCACTGTGTTTGCTGACGCAACCCCCACTGGTTGGGGCATTGCCACCACCTGTCAGCTCCTTTCCGGGACTTTCGCTTTCCCCCTCCCTATTG
	CCACGGCGGAACTCATCGCCGCCTGCCTTGCCCGCTGCTGGACAGGGGCTCGGCTGTTGGGCACTGACAATTCCGTGGTGTTGTCGGGGAAGCTGACGTCCTTTCCATGGCTGCTCGCCTGTGTTGCCACCTGGATTCTGCGCGGGACG
	TCCTTCTGCTACGTCCCTTCGGCCCTCAATCCAGCGGACCTTCCTTCCCGCGGCCTGCTGCCGGCTCTGCGGCCTCTTCCGCGTCTTCGCCTTCGCCCTCAGACGAGTCGGATCTCCCTTTGGGCCGCCTCCCCGCCTGG] [AAACGGG
	GGAGGCTAACTGAAACACGGAAGGAGACAATACCGGAAGGAACCCGCGCTATGACGGCAATAAAAAGACAGAATAAAACGCACGGGTGTTGGGTCGTTTGTTCATAAACGCGGGGTTCGGTCCCAGGGCTGGCACTCTGTCGATACCCC
	ACCGAGACCCCATTGGGGCCAATACGCCCGCGTTTCTTCCTTTTCCCCACCCCACCCCCCAAGTTCGGGTGAAGGCCCAGGGCTCGCAGCCAACGTCGGGGCGGCAGGCCCTGCCATAGC] [AGATCTGCGCAGCTGGGGCT]

Linear expression cassettes For IGKC(kappa)

CMV-FP_Primer	[AGATATACGCGTTGACATTG] [ATTATTGACTAGTTATTAATAGTAATCAATTACGGGGTCATTAGTTCATAGCCCATATATGGAGTTCCGCGTTACATAACTTACGGTAAATGGCCCGCCTGGCTGACCGCCCAACGACCCCCGCCC
CMV promoter	ATTGACGTCAATAATGACGTATGTTCCCATAGTAACGCCAATAGGGACTTTCCATTGACGTCAATGGGTGGAGTATTTACGGTAAACTGCCCACTTGGCAGTACATCAAGTGTATCATATGCCAAGTACGCCCCCTATTGACGTCAATG
CMV-RP_Primer	ACGGTAAATGGCCCGCCTGGCATTATGCCCAGTACATGACCTTATGGGACTTTCCTACTTGGCAGTACATCTACGTATTAGTCATCGCTATTACCATGGTGATGCGGTTTTGGCAGTACATCAATGGGCGTGGATAGCGGTTTGACTCA
K20_Primer	CGGGGATTTCCAAGTCTCCACCCCATTGACGTCAATGGGAGTTTGTTTTGGCACCAAAATCAACGGGACTTTCCAAAATGTCGTAACAACTCCGCCCCATTGACGCAAATGGGCGGTAGGCGTGTACGGTGGGAGGTCTATATAAGCAG
hman IGHG1 Constant region	AGCTCGTTTAGTGAACCGTCAGATCGCCTGGAGACGCCATCCACGCTGTTTTGACCTCCA] TAGAAGACACCGGGACCGATCCAGCCTCCGGACTCTAGACTTCGAATTCTGCAGTCGA [CGGTACCGCGGGCCCGGGA] [2nd-PCR
WPRE	product] [CGAACTGTGGCTGCACCATC] [TGTCTTCATCTTCCCGCCATCTGATGAGCAGTTGAAATCTGGAACTGCCTCTGTTGTGTGCCTGCTGAATAACTTCTATCCCAGAGAGGCCAAAGTACAGTGGAAGGTGGATAACGCC
poly(A) signal	CTCCAATCGGGTAACTCCCAGGAGAGTGTCACAGAGCAGGACAGCAAGGACAGCACCTACAGCCTCAGCAGCACCCTGACGCTGAGCAAAGCAGACTACGAGAAACACAAAGTCTACGCCTGCGAAGTCACCCATCAGGGCCTGAGCTC
WPRE_RP_Primer	GCCCGTCACAAAGAGCTTCAACAGGGGAGAGTGTTAG] GAATTCGCGGCCGCGAGTTTGATATCT [CGACAATCAACCTCTGGATTACAAAATTTGTGAAAGATTGACTGGTATTCTTAACTATGTTGCTCCTTTTACGCTATGTGGAT
	ACGCTGCTTTAATGCCTTTGTATCATGCTATTGCTTCCCGTATGGCTTTCATTTTCTCCTCCTTGTATAAATCCTGGTTGCTGTCTCTTTATGAGGAGTTGTGGCCCGTTGTCAGGCAACGTGGCGTGGTGTGCACTGTGTTTGCTGAC
	GCAACCCCCACTGGTTGGGGCATTGCCACCACCTGTCAGCTCCTTTCCGGGACTTTCGCTTTCCCCCTCCCTATTGCCACGGCGGAACTCATCGCCGCCTGCCTTGCCCGCTGCTGGACAGGGGCTCGGCTGTTGGGCACTGACAATTC
	CGTGGTGTTGTCGGGGAAGCTGACGTCCTTTCCATGGCTGCTCGCCTGTGTTGCCACCTGGATTCTGCGCGGGACGTCCTTCTGCTACGTCCCTTCGGCCCTCAATCCAGCGGACCTTCCTTCCCGCGGCCTGCTGCCGGCTCTGCGGC
	CTCTTCCGCGTCTTCGCCTTCGCCCTCAGACGAGTCGGATCTCCCTTTGGGCCGCCTCCCCGCCTGG] [AAACGGGGGAGGCTAACTGAAACACGGAAGGAGACAATACCGGAAGGAACCCGCGCTATGACGGCAATAAAAAGACAGAA
	TAAAACGCACGGGTGTTGGGTCGTTTGTTCATAAACGCGGGGTTCGGTCCCAGGGCTGGCACTCTGTCGATACCCCACCGAGACCCCATTGGGGCCAATACGCCCGCGTTTCTTCCTTTTCCCCACCCCACCCCCCAAGTTCGGGTGAA
	GGCCCAGGGCTCGCAGCCAACGTCGGGGCGGCAGGCCCTGCCATAGC] [AGATCTGCGCAGCTGGGGCT]

Linear expression cassettes For IGLC (lambda)

CMV-FP_Primer	[AGATATACGCGTTGACATTG] [ATTATTGACTAGTTATTAATAGTAATCAATTACGGGGTCATTAGTTCATAGCCCATATATGGAGTTCCGCGTTACATAACTTACGGTAAATGGCCCGCCTGGCTGACCGCCCAACGACCCCCGCCC
CMV promoter	ATTGACGTCAATAATGACGTATGTTCCCATAGTAACGCCAATAGGGACTTTCCATTGACGTCAATGGGTGGAGTATTTACGGTAAACTGCCCACTTGGCAGTACATCAAGTGTATCATATGCCAAGTACGCCCCCTATTGACGTCAATG
CMV-RP_Primer	ACGGTAAATGGCCCGCCTGGCATTATGCCCAGTACATGACCTTATGGGACTTTCCTACTTGGCAGTACATCTACGTATTAGTCATCGCTATTACCATGGTGATGCGGTTTTGGCAGTACATCAATGGGCGTGGATAGCGGTTTGACTCA
L20_Primer	CGGGGATTTCCAAGTCTCCACCCCATTGACGTCAATGGGAGTTTGTTTTGGCACCAAAATCAACGGGACTTTCCAAAATGTCGTAACAACTCCGCCCCATTGACGCAAATGGGCGGTAGGCGTGTACGGTGGGAGGTCTATATAAGCAG
hman IGHG1 Constant region	AGCTCGTTTAGTGAACCGTCAGATCGCCTGGAGACGCCATCCACGCTGTTTTGACCTCCA] TAGAAGACACCGGGACCGATCCAGCCTCCGGACTCTAGACTTCGAATTCTGCAGTCGA [CGGTACCGCGGGCCCGGGA] [2nd-PCR
WPRE	product] [GGTCAGCCCAAGGCTGCCCC] [CTCGGTCACTCTGTTCCCGCCCTCCTCTGAGGAGCTTCAAGCCAACAAGGCCACACTGGTGTGTCTCATAAGTGACTTCTACCCGGGAGCCGTGACAGTGGCCTGGAAGGCAGATAGC
poly(A) signal	AGCCCCGTCAAGGCGGGAGTGGAGACCACCACACCCTCCAAACAAAGCAACAACAAGTACGCGGCCAGCAGCTATCTGAGCCTGACGCCTGAGCAGTGGAAGTCCCACAGAAGCTACAGCTGCCAGGTCACGCATGAAGGGAGCACCGT
WPRE_RP_Primer	GGAGAAGACAGTGGCCCCTACAGAATGTTCATAG] GAATTCGCGGCCGCGAGTTTGATATCT [CGACAATCAACCTCTGGATTACAAAATTTGTGAAAGATTGACTGGTATTCTTAACTATGTTGCTCCTTTTACGCTATGTGGATACG
	CTGCTTTAATGCCTTTGTATCATGCTATTGCTTCCCGTATGGCTTTCATTTTCTCCTCCTTGTATAAATCCTGGTTGCTGTCTCTTTATGAGGAGTTGTGGCCCGTTGTCAGGCAACGTGGCGTGGTGTGCACTGTGTTTGCTGACGCA
	ACCCCCACTGGTTGGGGCATTGCCACCACCTGTCAGCTCCTTTCCGGGACTTTCGCTTTCCCCCTCCCTATTGCCACGGCGGAACTCATCGCCGCCTGCCTTGCCCGCTGCTGGACAGGGGCTCGGCTGTTGGGCACTGACAATTCCGT
	GGTGTTGTCGGGGAAGCTGACGTCCTTTCCATGGCTGCTCGCCTGTGTTGCCACCTGGATTCTGCGCGGGACGTCCTTCTGCTACGTCCCTTCGGCCCTCAATCCAGCGGACCTTCCTTCCCGCGGCCTGCTGCCGGCTCTGCGGCCTC
	TTCCGCGTCTTCGCCTTCGCCCTCAGACGAGTCGGATCTCCCTTTGGGCCGCCTCCCCGCCTGG] [AAACGGGGGAGGCTAACTGAAACACGGAAGGAGACAATACCGGAAGGAACCCGCGCTATGACGGCAATAAAAAGACAGAATAA
	AACGCACGGGTGTTGGGTCGTTTGTTCATAAACGCGGGGTTCGGTCCCAGGGCTGGCACTCTGTCGATACCCCACCGAGACCCCATTGGGGCCAATACGCCCGCGTTTCTTCCTTTTCCCCACCCCACCCCCCAAGTTCGGGTGAAGGC
	CCAGGGCTCGCAGCCAACGTCGGGGCGGCAGGCCCTGCCATAGC] [AGATCTGCGCAGCTGGGGCT]

Table S7. Gene family analysis of monoclonal antibodies

Number	Ab_ID	Heavy chain				Light chain		
		V-GENE and allele	D-GENE and allele	J-GENE and allele	CDR3-IMGT(aa)	V-GENE and allele	J-GENE and allele	CDR3-IMGT(aa)
1	81E8	IGHV2-70*15 F	IGHD6-13*01 F	IGHJ4*02 F	ARVQVAAAGSPYDY	IGKV1-39*01 F	IGKJ1*01 F	QQTYSTPRT
2	81D2	IGHV3-53*01 F	IGHD3-3*01 F	IGHJ4*02 F	ARFRYGDYPDY	IGKV1-33*01 F	IGKJ3*01 F	QQYDNLPSFT
3	81A2	IGHV4-34*01 F	IGHD2-2*02 F	IGHJ6*02 F	GVPYCSSSSCYRYYGMDV	IGKV1-9*01 F	IGKJ5*01 F	QQLNSYPQAT
4	81C8	IGHV3-33*01 F	IGHD3-3*01 F	IGHJ4*02 F	ARDGVDFGMVTLFDY	IGKV1-39*01 F	IGKJ1*01 F	QQSYNTPPWT
5	81A1	IGHV4-59*01 F	IGHD6-19*01 F	IGHJ3*02 F	ARDQGYSSGWNDAFDI	IGLV2-23*01 F	IGLJ3*02 F	CSYAGSRFWV
6	81A11	IGHV1-69*02 F	IGHD1-7*01 F	IGHJ2*01 F	AREAGTTDWYFDL	IGLV1-40*01 F	IGLJ2*01 F	QSYDSSLSVVV
7	81C3	IGHV4-39*01 F	IGHD3-3*01 F	IGHJ4*02 F	ARHPRFSWRGNDSGYFDY	IGLV2-14*01 F	IGLJ1*01 F	SSFTSSSTPYV
8	81C7	IGHV2-5*02 F	IGHD3-10*01 F	IGHJ4*02 F	AHSMVRGVLFGADFDY	IGLV1-36*01 F	IGLJ3*02 F	AAWDDSLNGPV
9	81D5	IGHV5-51*01 F	IGHD1-26*01 F	IGHJ3*02 F	ARRWDGVGFDI	IGLV3-19*01 F	IGLJ1*01 F	NSRDSSINHYV
10	81F2	IGHV4-34*01 F	IGHD1-14*01 ORF	IGHJ5*02 F	ARGWTVPPLWVLNWFDP	IGKV2-28*01 F	IGKJ4*01 F	MQALQTPRT
11	81G8	IGHV3-7*05 F	IGHD4-23*01 ORF	IGHJ4*02 F	ARSPHYYGGFDY	IGLV6-57*02 F	IGLJ3*02 F	QSYHNSVWV
12	81E1	IGHV1-24*01 F	IGHD3-10*01 F	IGHJ4*02 F	AITSVARGLRGYFDT	IGLV1-47*01 F	IGLJ2*01 F	AAWDDSLSRVV
13	81E10	IGHV1-24*01 F	IGHD3-10*01 F	IGHJ4*02 F	AITSLARGLKGYFDS	IGLV1-47*01 F	IGLJ2*01 F	AAWDDSLSGVI
14	81A6	IGHV3-9*01 F	IGHD2-2*01 F	IGHJ6*02 F	AKDIGCSSTSCSYYHYYGMDV	IGKV2-28*01 F	IGKJ2*01 F	MQALQTPT
15	81B2	IGHV3-66*02 F	IGHD6-19*01 F	IGHJ4*02 F	ARDGRAVAGTD	IGKV1-33*01 F	IGKJ1*01 F	HQYDNLPRT
16	81B7	IGHV1-18*04 F	IGHD3-10*01 F	IGHJ4*02 F	ARDYGWFGELSTEGQFDY	IGKV3-11*01 F	IGKJ3*01 F	QQRRDFT
17	82A6	IGHV4-39*01 F	IGHD6-19*01 F	IGHJ4*02 F	ARFITDGYSSGSDS	IGKV1-39*01 F	IGKJ4*01 F	QQSYSTPRLT
18	82C4	IGHV1-58*01 F	IGHD1-26*01 F	IGHJ6*02 F	AADRMRIVGGKGYYYGMDV	IGKV1-5*03 F	IGKJ2*01 F	QQYNSYSPGDT
19	82G8	IGHV4-59*08 F	IGHD2-15*01 F	IGHJ5*02 F	ARRSMGYCSGGNCYSGFDP	IGKV1-39*01 F	IGKJ4*01 F	QQSYSTPLT
20	82B6	IGHV4-61*04 F	IGHD3-16*01 F	IGHJ5*02 F	AMTYYDYIWGRVDPQFDP	IGKV2-30*01 F	IGKJ1*01 F	CMQGTHWPPT
21	82B7	IGHV1-18*04 F	IGHD3-10*01 F	IGHJ4*02 F	ARDYGWFGELSTEGQFDY	IGKV3-20*01 F	IGKJ1*01 F	HQYASSPRT
22	82C6	IGHV4-39*01 F	IGHD6-19*01 F	IGHJ4*02 F	ARFITDGYSSGSDS	IGKV2-30*02 [F]	IGKJ2*01 F	MQGTHWPMYT
23	82F6	IGHV3-30*03 F	IGHD2-15*01 F	IGHJ4*02 F	AKQASPYCSGGSCYSGNFDY	IGKV1-33*01 F	IGKJ4*01 F	QQHDNVPLT
24	82A5	IGHV1-18*04 F	IGHD3-9*01 F	IGHJ4*02 F	ARVQWLRLDY	IGKV1-12*01 F	IGKJ4*01 F	QQAKGFPLT
25	82C12	IGHV2-5*02 F	IGHD3-3*01 F	IGHJ4*02 F	AHRPAGFWSAHFDY	IGKV1-39*01 F	IGKJ1*01 F	QQSYSTPAWT
26	51D3	IGHV3-66*01 F	IGHD1-26*01 F	IGHJ6*02 F	AREGLLVGPTGRGLGMDV	IGKV1-33*01 F	IGKJ2*01 F	QQYADLPYT
27	51D4	IGHV2-70*15 F	IGHD3-10*01 F	IGHJ4*02 F	ARMVVRGVMLDY	IGKV1-39*01 F	IGKJ2*03 (F)	QQSYSPPHS
28	51A3	IGHV1-18*04 F	IGHD3-10*01 F	IGHJ4*02 F	ARDLAWFGELSESPIEY	IGKV3-11*01 F	IGKJ5*01 F	QQRGNSIT
29	51D2	IGHV2-5*01 F	IGHD3-9*01 F	IGHJ3*01 F	AHRLAPDYDFLTGYYNGDDAFDV	IGKV1-39*01 F	IGKJ4*01 F	QQSYNTLALS
30	51A1	IGHV3-66*01 F	IGHD5-12*01 F	IGHJ3*02 F	ARDLNIAGGFDI	IGKV1-9*01 F	IGKJ5*01 F	QHLNIDPIT
31	51E12	IGHV3-7*01 F	IGHD2-2*01 F	IGHJ4*02 F	ARLMYYYGNFDY	IGKV1-8*01 F	IGKJ2*01 F	QQYYGYPT
32	51D12	IGHV5-10-1*03 F	IGHD2-2*01 F	IGHJ6*02 F	ARLPFCDSASCGRAHYYYGMDV	IGKV3-15*01 F	IGKJ2*01 F	QQYNNWPET
33	51F11	IGHV1-69*04 F	IGHD5-18*01 F	IGHJ4*02 F	ATGRYTYGYGYYFDY	IGKV3-20*01 F	IGKJ2*02 (F)	QQYGSSRT
34	51E10	IGHV1-18*04 F	IGHD6-13*01 F	IGHJ2*01 F	ARARQLVLNWYFDL	IGKV4-1*01 F	IGKJ4*01 F	QQYYITPQLT
35	51E7	IGHV3-13*01 F	IGHD3-10*01 F	IGHJ2*01 F	ARVGYYGSGSYPLYWYFDL	IGKV1-39*01 F	IGKJ1*01 F	QQSYSAPPWT
36	51D7	IGHV5-51*01 F	IGHD6-19*01 F	IGHJ3*02 F	ATRTGWTNDAFDI	IGKV1-39*01 F	IGKJ2*02 (F)	QQSYSTPCT
37	51F5	IGHV2-70*13 F	IGHD1-7*01 F	IGHJ4*02 F	ALGRAGTMDY	IGKV1-39*01 F	IGKJ2*01 F	QQSYSPPYT
38	51E3	IGHV3-9*01 F	IGHD6-19*01 F	IGHJ6*02 F	AKDMVAGPHYYGMDV	IGLV1-44*01 F	IGLJ3*02 F	AAWDDSLNGWV
39	51B1	IGHV5-51*01 F	IGHD3-10*01 F	IGHJ6*02 F	ARHPSNFYDSGGDYYAMDV	IGLV2-23*02 F	IGLJ3*02 F	CSYAGSSSWV
40	52C1	IGHV3-66*01 F	IGHD3-10*01 F	IGHJ4*02 F	ARLASDGSGSYLDYFDY	IGLV1-40*01 F	IGLJ3*02 F	QSYDSSLSGSWV
41	52G1	IGHV3-9*01 F	IGHD6-19*01 F	IGHJ4*02 F	AKDLSSGWDLFDY	IGLV3-21*04 F	IGLJ2*01 F	QVWDTSGDPLV
42	52C6	IGHV1-69*01 F	IGHD1-26*01 F	IGHJ6*02 F	ATDGGGGSYYYAHYYYGMDV	IGLV8-61*01 F	IGLJ2*01 F	VLYMGSGIVV
43	52E7	IGHV5-51*01 F	IGHD4-17*01 F	IGHJ4*02 F	VRSDGDYVIGHDY	IGLV1-44*01 F	IGLJ3*02 F	ATWDDSLNGRV
44	52B6	IGHV3-48*03 F	IGHD4-17*01 F	IGHJ4*02 F	ARGRDDYGDYRGGDFDY	IGKV3-11*01 F	IGKJ3*01 F	QQRSNWPPIT
45	52F7	IGHV3-9*01 F	IGHD2-2*01 F	IGHJ6*02 F	AKDIGVMVPGVTPYGMDV	IGKV2D-30*01 F	IGKJ2*02 (F)	MQGTHWPPGT
46	52B8	IGHV1-69*01 F	IGHD3-10*01 F	IGHJ3*02 F	ARGPAYVSGTYYWNAFDI	IGKV3-15*01 F	IGKJ2*01 F	QHYNNWPLYT
47	52E9	IGHV3-30*04 F	IGHD6-13*01 F	IGHJ3*02 F	ARDPPPGNMGSMAQHLVLLVVFDI	IGKV1-39*01 F	IGKJ4*01 F	QQSYTTLALT
48	52G9	IGHV3-66*01 F	IGHD6-25*01 F	IGHJ6*02 F	ARDPMRPGMDV	IGKV1-33*01 F	IGKJ1*01 F	QQYDNLPRT
49	53H3	IGHV3-66*01 F	IGHD4-17*01 F	IGHJ3*02 F	ARYYGPQGRAFDI	IGKV1-33*01 F	IGKJ3*01 F	QQYDNLPLT
50	53C5	IGHV1-69*09 F	IGHD5-18*01 F	IGHJ4*02 F	ARGRYTYGTEGYFDN	IGKV1-5*01 F	IGKJ2*01 F	QQYNNLYT
51	53G1	IGHV3-33*03 F	IGHD6-19*01 F	IGHJ4*02 F	AKGGFGYASGWYYLDY	IGKV1-33*01 F	IGKJ5*01 F	QQYGNLPPIA
52	53B2	IGHV3-13*01 F	IGHD3-22*01 F	IGHJ4*02 F	ARAYYDTSGYYNYFDH	IGKV3-15*01 F	IGKJ2*01 F	QHYNNWPLYT
53	53H5	IGHV3-53*01 F	IGHD3-10*01 F	IGHJ5*02 F	ARGYGSGSYGWFDP	IGKV3-15*01 F	IGKJ2*01 F	QHYNNWPLYT
54	53H6	IGHV3-53*04 F	IGHD1-26*01 F	IGHJ6*02 F	AREGLGMDV	IGKV3-15*01 F	IGKJ2*01 F	QHYNNWPLYT
55	53F9	IGHV3-53*04 F	IGHD1-26*01 F	IGHJ4*02 F	AREGLVGTTLTFDY	IGKV2D-30*01 F	IGKJ2*02 (F)	MQGTHWPPGT
56	53G6	IGHV2-70*15 F	IGHD1-26*01 F	IGHJ5*02 F	ARFLVGGFKAWFDP	IGLV1-51*01 F	IGLJ3*02 F	GTWDTSLNVWV
57	53C10	IGHV3-43*02 F	IGHD1-20*01 F	IGHJ4*02 F	ARESPKLTGYFDY	IGLV3-21*02 F	IGLJ1*01 F	QVWDSSSDPYV
58	53E11	IGHV1-46*01 F	IGHD5-12*01 F	IGHJ4*02 F	ARDQAFIVATLGPDY	IGLV8-61*01 F	IGLJ3*02 F	VLYMGSGIWV
59	53E12	IGHV3-53*01 F	IGHD5-12*01 F	IGHJ5*02 F	AKMLWLRGWFDP	IGLV6-57*03 F	IGLJ3*02 F	QSYDTSNHWV
60	53F12	IGHV3-66*01 F	IGHD4-23*01 ORF	IGHJ6*02 F	ARDAVGSYYYGMEV	IGKV3-15*01 F	IGKJ2*01 F	QHYNNWPLYT
61	54H2	IGHV5-51*01 F	IGHD6-19*01 F	IGHJ4*02 F	ARQESGWSFDY	IGKV1-39*01 F	IGKJ1*01 F	QQSYSTPRT
62	54F10	IGHV3-53*04 F	IGHD5-24*01 ORF	IGHJ6*02 F	ARDLEERGAMDV	IGKV3-20*01 F	IGKJ1*01 F	QQYGSSLWT
63	54G7	IGHV3-66*01 F	IGHD3-16*02 F	IGHJ5*02 F	ARAGWLRGRFDP	IGLV3-21*02 F	IGLJ3*02 F	QVWDSTTDLPHWV
64	55G3	IGHV2-70*15 F	IGHD1-14*01 ORF	IGHJ3*02 F	ARTRLGITAFDI	IGKV1-39*01 F	IGKJ1*01 F	QQSYTTPRT
65	55A8	IGHV1-69*04 F	IGHD4-17*01 F	IGHJ4*02 F	ARGTEYGDYDVSHD	IGKV1-5*03 F	IGKJ2*01 F	QQYNSYSHT
66	55C9	IGHV3-53*04 F	IGHD2-15*01 F	IGHJ4*02 F	AREGLVGTALAFDY	IGKV1-39*01 F	IGKJ2*01 F	QQSYSTPPYT
67	55G9	IGHV3-13*01 F	IGHD3-22*01 F	IGHJ2*01 F	ARVGYDSSGYYWYLDL	IGKV1-39*01 F	IGKJ3*01 F	QQSYTTPLFT
68	55G11	IGHV3-30*03 F	IGHD2-15*01 F	IGHJ4*02 F	GKGAGPYCGGGSCYPTKVDY	IGKV1-33*01 F	IGKJ1*01 F	QQYDNLLWT
69	56C3	IGHV3-33*01 F	IGHD3-10*01 F	IGHJ4*02 F	AKDGSGSYYNSGALDY	IGKV1-33*01 F	IGKJ2*01 F	QQYDNLPPYT
70	56H3	IGHV3-66*01 F	IGHD4-17*01 F	IGHJ4*02 F	ARDYGDYYFDY	IGKV3-20*01 F	IGKJ1*01 F	QQYGSSPRT
71	56B4	IGHV1-18*01 F	IGHD2-2*01 F	IGHJ4*02 F	ATDDPDIVLVPAAMSLDY	IGKV1-39*01 F	IGKJ4*01 F	QQSYNTLALS
72	56D7	IGHV3-66*01 F	N.D.	IGHJ6*02 F	ARDLDYYGMDV	IGKV1-9*01 F	IGKJ5*01 F	QQLNSYPPIT
73	56H7	IGHV4-59*01 F	IGHD3-22*01 F	IGHJ6*02 F	ATDYYDSSGYRYGMDV	IGKV1D-12*01 F	IGKJ4*01 F	QQANSFPLT
74	56A8	IGHV1-69*01 F	IGHD1-26*01 F	IGHJ4*02 F	ASFGSLWDLRDY	IGKV3-20*01 F	IGKJ4*01 F	QQYGTSRT
75	56E8	IGHV3-23*01 F	IGHD2-15*01 F	IGHJ4*02 F	AKDVGSRLIYDVFDY	IGKV1-39*01 F	IGKJ2*03 (F)	QQSYSTPPYS
76	56A10	IGHV2-70*15 F	IGHD4-23*01 ORF	IGHJ4*02 F	TRTATVVKDY	IGKV1-39*01 F	IGKJ1*01 F	QQSYSTPRT
77	56B11	IGHV2-70*15 F	IGHD6-6*01 F	IGHJ4*02 F	ARMIPIPALDY	IGKV1-39*01 F	IGKJ2*01 F	QQSYSTPHT
78	56B12	IGHV2-70*15 F	IGHD6-13*01 F	IGHJ4*02 F	AREEAAGTKLDY	IGKV1-39*01 F	IGKJ1*01 F	QQSYSTPRT
79	56C12	IGHV3-30*03 F	IGHD2-15*01 F	IGHJ5*02 F	AKDPTSLYCSGGSCYNNWFDP	IGKV1-39*01 F	IGKJ1*01 F	QQTYSTPRT
80	56E1	IGHV3-30*04 F	IGHD3-16*01 F	IGHJ3*02 F	AGGGVLVTSDPDAFDI	IGLV1-44*01 F	IGLJ3*02 F	AAWDDSLNGWV
81	56A3	IGHV3-30*03 F	IGHD2-15*01 F	IGHJ4*02 F	AKRGGTYCSGGICYGGYFDY	IGLV1-40*01 F	IGLJ3*02 F	QSYDSSLSDWGV
82	56F3	IGHV1-46*01 F	IGHD3-10*01 F	IGHJ4*02 F	ARDYSRITMIRGAGDY	IGLV1-51*01 F	IGLJ3*02 F	GTWDSSLSAQV
83	56H9	IGHV3-53*04 F	IGHD6-13*01 F	IGHJ5*02 F	ARGPYPSSSWA	IGLV2-14*01 F	IGLJ1*01 F	SSFTSSSTPYV
84	56H11	IGHV4-4*07 F	IGHD5-12*01 F	IGHJ4*02 F	AGEQHIVTTIIDY	IGLV1-44*01 F	IGLJ3*02 F	ATWDDSLNGRV
85	57B2	IGHV3-30*04 F	IGHD3-16*01 F	IGHJ3*02 F	AGGGVLVTSDPDAFDI	IGKV1-33*01 F	IGKJ3*01 F	QQSDNVPVT
86	57C4	IGHV3-15*01 F	IGHD4-17*01 F	IGHJ5*01 F	STTNDYGDYSANY	IGKV1-39*01 F	IGKJ4*01 F	QQSYSTPLT
87	57E7	IGHV5-51*01 F	IGHD3-22*01 F	IGHJ4*02 F	ARIEYYNDSSGYYQF	IGKV3-20*01 F	IGKJ1*01 F	QQYGSSWT
88	57H7	IGHV1-8*02 F	IGHD3-10*01 F	IGHJ5*02 F	ARGLWFGDLTRTKYNWFDP	IGKV1D-13*01 F	IGKJ4*01 F	QQFNNFLLT
89	57A8	IGHV3-23*01 F	IGHD1-26*01 F	IGHJ4*02 F	AKGQRGSPDFFDY	IGKV1-5*03 F	IGKJ4*01 F	QQYNSYSPLT
90	57B8	IGHV3-53*01 F	IGHD2-21*02 F	IGHJ4*02 F	ARDLVTWGLDY	IGKV1-9*01 F	IGKJ5*01 F	QLLNTDPIT
91	57A9	IGHV1-3*04 (F)	IGHD1-26*01 F	IGHJ4*02 F	ARAGWELNY	IGKV4-1*01 F	IGKJ1*01 F	QQYYSFWA
92	57G9	IGHV2-70*15 F	IGHD6-6*01 F	IGHJ4*02 F	ARITPHLVYDY	IGKV1-39*01 F	IGKJ2*02 (F)	QQSYSIPRT
93	57A6	IGHV5-51*01 F	IGHD6-19*01 F	IGHJ4*02 F	ARQESGWSFDY	IGLV3-19*01 F	IGLJ3*02 F	NSRDSSGNHWV
94	57F7	IGHV4-34*01 F	IGHD6-6*01 F	IGHJ6*02 F	ARDDSSSSGVGTGMDV	IGLV1-44*01 F	IGLJ3*02 F	AVWDDSLNGWV
95	57F8	IGHV2-5*02 F	IGHD3-10*01 F	IGHJ5*02 F	AHTTWYYYGSGWFDP	IGLV1-44*01 F	IGLJ2*01 F	AAWDDSLNGHV
96	57A11	IGHV1-18*01 F	IGHD3-10*01 F	IGHJ5*02 F	ARVQEFWLDP	IGLV3-21*04 F	IGLJ3*02 F	QVWDSSSDHPL
97	57E11	IGHV1-8*02 F	IGHD3-10*01 F	IGHJ5*02 F	ARGLWFGDLTRTKYNWFDP	IGLV1-44*01 F	IGLJ3*02 F	AAWDDSLNGWV
98	58G1	IGHV3-53*01 F	IGHD4-17*01 F	IGHJ6*02 F	ARDLENGGLDV	IGKV1D-12*01 F	IGKJ4*01 F	QQTNSFPT
99	58D2	IGHV3-11*01 F	IGHD3-10*01 F	IGHJ2*01 F	ASPLLSHNYGSGSYYNVYWYFEL	IGKV3-11*01 F	IGKJ2*02 (F)	QQLGT
100	58A4	IGHV4-59*01 F	IGHD3-9*01 F	IGHJ5*02 F	ARTLGAYYDILTGFRTPGGWFAP	IGKV3-20*01 F	IGKJ1*01 F	QQYGSSPWT
101	58B5	IGHV3-23*01 F	IGHD3-10*01 F	IGHJ4*02 F	AKEPSFGLWFGELSG	IGKV3-20*01 F	IGKJ2*01 F	QQYGSSLPYT
102	58G6	IGHV1-58*01 F	IGHD2-2*01 F	IGHJ3*02 F	AAPNCNSTTCHDGFDI	IGKV3-20*01 F	IGKJ1*01 F	QQYDNSPWT
103	58G9	IGHV3-13*04 F	IGHD3-9*01 F	IGHJ3*02 F	ARGSLRGGILSGYAFDI	IGKV1-39*01 F	IGKJ1*01 F	QQSYSSPPWT
104	58E2	IGHV4-39*07 F	IGHD3-10*01 F	IGHJ3*02 F	ARYYGPGTYYDAFDI	IGLV2-14*01 F	IGLJ3*02 F	SSYTSSSTWV
105	58A3	IGHV3-30*04 F	IGHD3-10*01 F	IGHJ4*02 F	ARDWVHYGSGSYPPDY	IGLV2-18*02 F	IGLJ3*02 F	SSYTSSSTWV
106	58H3	IGHV5-51*01 F	IGHD3-10*01 F	IGHJ4*02 F	ARHPVLRGNIDY	IGLV1-40*01 F	IGLJ3*02 F	QSYDSSLRGSV
107	510H2	IGHV3-66*01 F	IGHD5-12*01 F	IGHJ4*02 F	ARDKWEGTFDY	IGKV1-9*01 F	IGKJ4*01 F	QQLNSYPRMT
108	510A4	IGHV2-70*15 F	IGHD6-13*01 F	IGHJ4*02 F	ARVQVAAAGSPYDY	IGKV2-28*01 F	IGKJ1*01 F	MQALQMGT

109	510G4	IGHV4-31*03 F	IGHD4-23*01 ORF	IGHJ4*02 F	ARDYGGNSNYFHY	IGKV1-33*01 F	IGKJ4*01 F	QQYDTLPLT
110	510H4	IGHV3-66*01 F	IGHD5-18*01 F	IGHJ6*02 F	AETGWDGMDV	IGKV3-11*01 F	IGKJ1*01 F	QQRSNWPGT
111	510A5	IGHV3-9*01 F	IGHD3-9*01 F	IGHJ4*02 F	AKDRGYEILTPASFDY	IGKV1-39*01 F	IGKJ2*01 F	QQSYSTPPYT
112	510F6	IGHV2-5*02 F	IGHD5-18*01 F	IGHJ4*02 F	AHSLPSKYSYSYGSFDY	IGKV1-39*01 F	IGKJ2*01 F	QQSYSAPYT
113	510D7	IGHV1-69*04 F	IGHD5-18*01 F	IGHJ4*02 F	ATGRYTYGYGYYFDY	IGKV3-20*01 F	IGKJ2*02 (F)	QQYGSSRT
114	510E10	IGHV3-23*01 F	IGHD3-10*01 F	IGHJ5*02 F	AKGELLWFGELLENWFDP	IGKV1-12*01 F	IGKJ1*01 F	QQADSFPWT
115	510H10	IGHV2-70*15 F	IGHD6-13*01 F	IGHJ4*02 F	ARIQRGIAADY	IGKV1-39*01 F	IGKJ2*02 (F)	QQSYSTPRT
116	510B1	IGHV5-51*01 F	IGHD3-10*01 F	IGHJ3*02 F	ARLPPHFGSGSYYGNAFDI	IGLV1-47*01 F	IGLJ3*02 F	ATWDDSLTGPV
117	510G2	IGHV7-4-1*02 F	IGHD3-10*01 F	IGHJ6*02 F	ASTVGRGSGTYYYGNYYSYSMDV	IGLV2-14*01 F	IGLJ2*01 F	TSYTGSSTSVV
118	510H7	IGHV4-59*08 F	IGHD6-13*01 F	IGHJ5*02 F	ARHCPWQQLVSNWFDP	IGKV1D-13*01 F	IGKJ4*01 F	QQFNNFLLT
119	510H6	IGHV1-46*01 F	IGHD3-3*01 F	IGHJ6*02 F	ARTGFLIPSKGGGMDV	IGLV2-14*01 F	IGLJ2*01 F	SSYTSSSSLQI
120	510C4	IGHV3-48*03 F	IGHD1-26*01 F	IGHJ4*02 F	ARDPGEWESLDLDY	IGLV1-40*01 F	IGLJ3*02 F	QSYDSSLSGNWV
121	511A1	IGHV4-31*03 F	IGHD6-13*01 F	IGHJ6*02 F	AREKIRSIAAAGTVYYYGMDV	IGKV3-15*01 F	IGKJ1*01 F	QQYNNWPPWT
122	511B4	IGHV4-59*08 F	IGHD3-22*01 F	IGHJ5*01 F	ASTYWDSSGYYYGVDY	IGKV1D-12*01 F	IGKJ4*01 F	QQANSFRLT
123	511E7	IGHV5-51*01 F	IGHD3-10*01 F	IGHJ4*02 F	ALAVGRGIPTSYFDY	IGKV1-33*01 F	IGKJ3*01 F	QQYHNLPIT
124	511G7	IGHV3-33*01 F	IGHD4-17*01 F	IGHJ4*02 F	AKGGNYGDYLRGFDY	IGKV1-33*01 F	IGKJ4*01 F	QQYHNVPPA
125	511E9	IGHV1-18*01 F	IGHD3-10*01 F	IGHJ4*02 F	AREGAGLIIAYDY	IGKV6-21*01 F	IGKJ2*01 F	HQSSSLPYT
126	511D11	IGHV1-18*01 F	IGHD2-15*01 F	IGHJ6*02 F	AVLDYCSGGSSSSGYYNYGMDV	IGKV3-20*01 F	IGKJ2*01 F	QQYGRSPYT
127	511H11	IGHV3-13*04 F	IGHD6-19*01 F	IGHJ6*03 F	VRGDHSSGWYGTYYYYMDV	IGKV1-39*01 F	IGKJ1*01 F	QQSYSSPPWT
128	511D12	IGHV3-66*01 F	IGHD5-12*01 F	IGHJ3*02 F	ARDLDIAGAFDI	IGKV1-9*01 F	IGKJ5*01 F	QLLNSFPIT
129	511A5	IGHV4-31*06 F	IGHD3-22*01 F	IGHJ2*01 F	ARIYRGTMVVVFSDLHWYFDL	IGLV3-21*04 F	IGLJ1*01 F	QVWDSSADHYV
130	511E5	IGHV1-2*02 F	IGHD3-16*01 F	IGHJ2*01 F	ARDSLFSRVDWYFDL	IGLV1-40*01 F	IGLJ2*01 F	NSRDSSGNTVV
131	511G5	IGHV1-46*01 F	IGHD6-6*01 F	IGHJ4*02 F	ARDGALYSNSPTEFDY	IGLV1-47*01 F	IGLJ3*02 F	TTWDASRGGWV
132	511B7	IGHV1-46*01 F	IGHD2-2*01 F	IGHJ4*02 F	ARGGLVPAVMPALDY	IGLV1-47*01 F	IGLJ3*02 F	AAWDDSLSGPV
133	511H7	IGHV3-23*01 F	IGHD3-22*01 F	IGHJ6*02 F	ARGLQYYYDTSGYYKDSYYYGVDV	IGLV1-47*01 F	IGLJ3*02 F	AAWDDSLSGPV
134	511B11	IGHV3-7*03 F	IGHD3-10*01 F	IGHJ4*02 F	AGLFWYGGYFDY	IGLV1-40*01 F	IGLJ1*01 F	QSYDRSLSVLYV
135	59B11	IGHV3-13*04 F	IGHD3-3*01 F	IGHJ6*03 F	ARGTQDRVELMVGSPYYYYYMDV	IGKV1-39*01 F	IGKJ2*01 F	QQSYITTMYT
136	59D6	IGHV4-34*01 F	IGHD3-22*01 F	IGHJ4*02 F	ARHRRDYITMIVRPTRLWAFDY	IGLV1-40*01 F	IGLJ2*01 F	QSYDSALVV
137	59A1	IGHV3-66*01 F	IGHD1-26*01 F	IGHJ4*02 F	ARELGPVGGTDQ	IGKV1-39*01 F	IGKJ2*01 F	QQSHSTPYT
138	59A2	IGHV3-66*01 F	IGHD2-15*01 F	IGHJ4*02 F	ARDLPLHGDYFDY	IGKV1-33*01 F	IGKJ3*01 F	QQSDNVPVT
139	59H6	IGHV3-30*04 F	IGHD2-15*01 F	IGHJ4*02 F	ARETLGGYCNGGSCYDAGYFDY	IGKV3-20*01 F	IGKJ1*01 F	QQYGSSPWT
140	59G12	IGHV3-33*01 F	IGHD3-3*01 F	IGHJ4*02 F	ARDGVDFGMVTLFDY	IGKV1-39*01 F	IGKJ1*01 F	QQSYNTPPWT
141	8B1E6	IGHV4-4*02 F	IGHD3-16*01 F	IGHJ4*02 F	ARVQGLIDY	IGKV1-NL1*01 F	IGKJ2*02 (F)	QQYYSTPPRT
142	8B1B1	IGHV5-51*01 F	IGHD6-13*01 F	IGHJ6*03 F	ASQAAAGYYYYMDV	IGKV1-39*01 F	IGKJ1*01 F	QQSYNILWT
143	8B1H12	IGHV3-23*01 F	IGHD4-17*01 F	IGHJ5*02 F	AKQTDYGVGWFDP	IGKV1-33*01 F	IGKJ4*01 F	QQYDNFSLT
144	8B1E11	IGHV1-69*06 F	IGHD3-10*01 F	IGHJ4*02 F	AVLPLHSSYNWYYFDY	IGKV3-11*01 F	IGKJ2*01 F	QQRSNWPPGMYT
145	8B2F2	IGHV2-5*02 F	IGHD6-13*01 F	IGHJ5*02 F	AHQRHSNSWYVSAWFDP	IGLV1-40*01 F	IGLJ1*01 F	QSYDSSLSGNFV
146	8B5A6	IGHV3-33*01 F	IGHD6-13*01 F	IGHJ4*02 F	AKGGWYSSKWYYFDY	IGKV2-28*01 F	IGKJ1*01 F	MQALQMGT
147	8B2D5	IGHV3-13*01 F	IGHD4-17*01 F	IGHJ3*02 F	ARGSDTVTTAFDI	IGKV1-39*01 F	IGKJ4*01 F	QQSYTTPGLT
148	8B2H8	IGHV3-53*04 F	IGHD3-10*01 F	IGHJ4*02 F	AREAPNSRGSGTNFDY	IGKV1-39*01 F	IGKJ2*01 F	QQSYSTPPYT
149	8B2D11	IGHV3-33*01 F	IGHD5-18*01 F	IGHJ4*02 F	AKNGYSYAYPRQYFDY	IGKV1-33*01 F	IGKJ2*02 (F)	QHYDNLKVT
150	8B2E4	IGHV4-31*03 F	IGHD3-10*01 F	IGHJ4*02 F	ARVSRYTMVRGVIFDY	IGLV2-23*02 F	IGLJ2*01 F	CLYAGHSTYVV
151	8B2G6	IGHV4-38-2*02 F	IGHD2-21*02 F	IGHJ4*02 F	ARVGVATILGVDY	IGLV6-57*03 F	IGLJ3*02 F	QSYDSSWV
152	8B2E12	IGHV3-30*03 F	IGHD6-19*01 F	IGHJ6*02 F	AKGGGYISAWSTRYYAMDV	IGLV2-14*01 F	IGLJ3*02 F	SSYTSSSTWV
153	8B3E9	IGHV3-23*01 F	IGHD6-13*01 F	IGHJ4*02 F	AESSSLTGNFNY	IGLV3-21*03 F	IGLJ3*02 F	QVWDTAWV
154	8B5A1	IGHV3-13*01 F	IGHD5-18*01 F	IGHJ4*02 F	ARGFDTTTGFYFDY	IGKV1-NL1*01 F	IGKJ1*01 F	QQDYNFPWT
155	8B5B6	IGHV1-69*04 F	IGHD3-10*01 F	IGHJ6*03 F	ARTEYSYDSGSSRAYSMDV	IGKV1-39*01 F	IGKJ1*01 F	QQTHSTPRT
156	8B5E5	IGHV7-4-1*02 F	IGHD6-13*01 F	IGHJ5*02 F	ARVGPSSSWPS	IGKV1-39*01 F	IGKJ1*01 F	QQSYSTPRT
157	8B5C1	IGHV3-33*01 F	IGHD6-13*01 F	IGHJ4*02 F	AKGGWYSSKWYYFDY	IGKV2-28*01 F	IGKJ1*01 F	MQALQMGT
158	8B5F7	IGHV3-7*01 F	IGHD3-3*01 F	IGHJ4*02 F	ARDLGVLWFGDPY	IGKV1-NL1*01 F	IGKJ1*01 F	QQYYSAPRT
159	8B4G4	IGHV2-5*02 F	IGHD3-9*01 F	IGHJ4*02 F	AHSPDHRYFDVLTGYFNSERFYFDY	IGLV1-51*01 F	IGLJ2*01 F	GTWDSSLSAGV
160	8B4A7	IGHV4-39*07 F	IGHD6-6*01 F	IGHJ6*02 F	ARIPRHLGQDHYYYVMDV	IGLV2-23*01 F	IGLJ1*01 F	CSYAGIFV
161	8B4D9	IGHV3-30*03 F	IGHD5-18*01 F	IGHJ4*02 F	AKAAGGGYSYIYWGGDY	IGLV6-57*03 F	IGLJ3*02 F	QSYDSSNLWV
162	8B4E1	IGHV4-61*01 F	IGHD2-2*01 F	IGHJ6*02 F	AREYFVSLPAAQTLYYYGIDV	IGKV3-15*01 F	IGKJ1*01 F	QQYKNWPPWT
163	8B4H2	IGHV1-8*02 F	IGHD3-10*01 F	IGHJ5*02 F	ARGLWFGDLTRTKYNWFDP	IGKV3-20*01 F	IGKJ4*01 F	HQYDSSPLT
164	8B4A3	IGHV1-46*01 F	IGHD3-10*01 F	IGHJ6*02 F	ARDPPSGNYDNIDEWTRSENHYNYGMDA	IGKV3-11*01 F	IGKJ4*01 F	QQRSNWPYLT
165	8B4C5	IGHV3-11*06 F	IGHD6-19*01 F	IGHJ4*02 F	ARDGSAVAGPMSYFDY	IGKV1-NL1*01 F	IGKJ1*01 F	QQYYSIPRT
166	8B4E5	IGHV2-70*15 F	IGHD6-19*01 F	IGHJ4*02 F	AREVAGAVHLDY	IGKV1-39*01 F	IGKJ1*01 F	QQSFSTPRT
167	8B4B6	IGHV3-7*03 F	N.D.	IGHJ4*02 F	ARDLGVLWFGDLLF	IGKV1-NL1*01 F	IGKJ1*01 F	QQYYSDPPRT
168	8B4E11	IGHV4-59*01 F	IGHD3-10*01 F	IGHJ4*02 F	ARGGYYYGPPRDFDY	IGKV3-20*01 F	IGKJ2*01 F	QHYGSSPQYT
169	13G9	IGHV1-58*01 F	IGHD2-2*01 F	IGHJ3*02 F	AAPYCSSTSCRDGFDI	IGKV3-20*01 F	IGKJ1*01 F	QQYGRSPWT